DOI:10.14753/SE.2025.3289

SEMMELWEIS EGYETEM

DOKTORI ISKOLA

Ph.D. értekezések

3289.

CSENDE KRISTÓF

Légzőszervi megbetegedések

című program

Programvezető: Dr. Müller Veronika, egyetemi tanár

Témavezető: Dr. Megyesfalvi Zsolt, tudományos munkatárs

DOI:10.14753/SE.2025.3289

Comprehensive analysis of tumor heterogeneity in neuroendocrine lung cancers

PhD thesis

Kristóf Csende

Semmelweis University Doctoral School

Rácz Károly Conservative Medicine Division

Supervisor: Zsolt Megyesfalvi, MD, D.Sc

Official reviewers: László Piros MD, Ph.D.
András Buzás MD, Ph.D.

Head of the Complex Examination Committee: Veronika Müller, MD, D.Sc

Members of the Complex Examination Committee: Attila Szabó, D.Sc
Péter Lakatos, D.Sc

Budapest
2025

DOI:10.14753/SE.2025.3289

Table of contents

DOI:10.14753/SE.2025.3289

List of Abbreviations

AC, Atypical carcinoid

ACTH, Adrenocorticotropic hormone

ASCL1, Achaete-Scute Homologue 1

CAR-T, Chimeric antigen receptor T-cell

ChT, Chemotherapy

CPM, counts per million

DAB, 3-3′-diaminobenzidine

DLL3, Delta-like ligand 3

EZH2, enhancer of zeste homolog 2

FC, Fold-changes

FFPE, Formalin-fixed, paraffin-embedded

H&E, Hematoxylin and eosin

HPFs, High-power fields

H_2O_2, Hydrogen peroxid

IASLC, International Association for the Study of Lung Cancer

ICOS, Inducible T-cell costimulator

IC, Immune cell

IDO, Indolamine 2,3-dioxygenase

IHC, Immunohistochemistry

LAG3, Lymphocyte-activation gene 3

LCNEC, Large cell neuroendocrine carcinoma

LN, Lymph node

LNEC, Lung neuroendocrine carcinoma

LNEN, Lung neuroendocrine neoplasm

LNET, Lung neuroendocrine tumor

LSD1, Lysine-specific demethylase

myc, myc proto-oncogenes

mTOR, mammalian target of rapamycin proteins

NE, Neuroendocrine

NEUROD1, Neurogenic differentiation factor 1

NCCN, National Comprehensive Cancer Network

NKG2A, CD94/NK Group 2 Member A

NSCLC, Non-small cell lung cancer

ORR, Overall response rate

OS, Overall survival

OX40, Tumor necrosis factor receptor superfamily, member 4

PCA, Principal component analysis

PD-1, Programmed cell death protein 1

PD-L1, Programmed death-ligand 1

PFS, Progression-free survival

PGC-1α, Peroxisome proliferator-activated receptor gamma coactivator 1-alpha

PIK3, Phosphoinositide 3-kinase

POU2F3, POU class 2 hoemobox 3

PT, Primary tumor

RNA, Ribonucleic acid

RNAseq, RNA sequencing

RT, Radiotherapy

SCLC, Small cell lung cancer

SCLC-A, Small cell lung cancer ASCL1-subtype

SCLC-AN, Small cell lung cancer ASCL1/NEUROD1-subtype

SCLC-I, Small cell lung cancer inflammatory-subtype

SCLC-N, Small cell lung cancer NEUROD1-subtype

SCLC-P, Small cell lung cancer POU2F3-subtype

SCLC-QN, Small cell lung cancer quadruple-negative SCLC subtype

SIADH, Syndrome of inappropriate antidiuretic-hormone

SSA, Somatostatin analogues

TC, Typical carcinoid

TCs, Tumor cells

TIM, Tumor immune microenvironment

TMA, Tissue microarray

VEGFs, vascular endothelial growth factors

YAP1, Yes-associated protein 1

1. Introduction

1.1. Epidemiology

Lung cancer was the leading cause of cancer-related deaths in 2022, accounting for an estimated 1.8 million deaths. This represents 18.7% of all cancer types globally. Hungary had the highest incidence of respiratory malignancy among women, and this number has not decreased over the last decade. (1, 2) A commonly overlooked fact is that in Europe, these types of cancers are the second leading cause of maternal orphanhood (11-18%). (3) The loss of a parent has a profound and lasting negative impact on both the child and society. (4-6)

The two main categories of lung cancer are described as: non-small cell lung cancer (NSCLC), which accounts for ≈80-85% of lung cancer cases, and small cell lung cancer (SCLC), which represents ≈10-15% of cases, although there are also some other rare categories of lung malignancies which can add upto ≈5%. (7, 8) SCLC has the worst prognosis, with a 5-year mortality rate of 90% or more. (9) A common histological origin of lung cancers, formed from the bronchial and bronchiolar epithelium, is known as Kulchitsky cells or neuroendocrine (NE) cells. (10) Nevertheless, the precursor cells of SCLC tumorigenesis differ, as SCLCs can occur from different cellular entities: NE cells, type 2 alveolar cells, tuft cells, and even epidermal growth factor receptor (EGFR)-driven, ALK-driven, or RET-driven lung adenocarcinomas. (11) The recent 2021 WHO Lung cancer classification divided lung NE neoplasm (LNEN) into well-differentiated lung NE tumors (LNET) and poorly differentiated lung NE carcinomas (LNEC). LNET is further separated into typical carcinoid (TC) and atypical carcinoid (AC), while LNEC comprises large-cell neuroendocrine carcinoma (LCNEC) and SCLC. (12, 13) From another aspect, lung tumors can also be distributed as 20-25% NE tumors and 75% NSCLC. (14) Besides SCLC, LNENs are rare as TC accounts for around 1-2% of all lung cancers, while AC is the rarest with an incidence of less than 0.2%. The LCNEC and SCLC represent 2-3% and 10-15% of lung cancers, respectively. The incidence of TC, AC, and LCNEC has been increasing over the past decade. It is unclear, however, whether this trend is caused by improved clinical practice in diagnosis or we actually have a growing number of cases. The incidence of SCLCs are decreasing, probably resulting from a drop in smoking prevalence and improved prevention. (15-18) Disease progression and treatment response differ between each subtype due to their unique characteristics. (19) At the time of the

diagnosis, TC patients have a mean age of 45 years, with a higher prevalence in females, while AC patient's mean age is between 55-60, with an equal gender distribution. LCNEC and SCLC are more frequent in the older, smoking male population, with a mean age of 65-75. (20-22) TC is not directly linked with smoking, showing a different biological behavior compared to the other subtypes. On the other hand, AC is also strongly associated with smoking, alongside the previously mentioned LCNEC and SCLC. (20-22) This constant carcinogen exposure leads to a high mutation rate, which inactivates tumor suppressor genes *TP53* and *RB1*. These genetic alterations play a significant role in the development and aggressiveness of the tumor. (23-26)

1.2. Biological properties and diagnosis

LNENs are diverse. The subtypes differ in grade, appearance, mitotic activity, and necrosis. (27) TCs are well-differentiated NE tumors with a low grade and low proliferative activity by fewer than two mitoses per 2 mm^2 or 10 high-power fields (HPFs). In contrast, AC has intermediate characteristics between TC and LNEC. ACs are still well-differentiated tumors but have higher mitotic activity, ranging from 2 to 10 mitoses per 2 mm^2 / 10 HPFs, and focal necrosis. LCNEC and SCLC are classified as LNEC, showing similar aggressive clinical features. LCNEC typically shows over 10 mitoses per 2 mm^2 / 10 HPFs, with a median count of 70, and extensive necrosis is present. SCLC is considered even more aggressive than LCNEC, with a higher median mitotic count of 80 per 2 mm^2 / 10 HPFs, and presents extensive necrosis. (28) Necrosis and mitotic activity are one of the key measurements to differentiate between LNENs. A recent study addresses the fact that HPF is an outdated system. Mitoses should always be counted in regions of peak activity and recorded as the number of occurrences per 2 mm^2. These findings have already been implemented in the newest WHO classification of lung tumors (2021). The classification range stayed the same, but the counting method and the unit of measurement changed. (12, 29)

The Ki-67 index can be an effective tool for separating carcinoids from high-grade tumors such as SCLC and LCNEC, but its role in clinical practice is not well defined. (30-33)

Patients with LNET often experience symptoms, including cough, hemoptysis, and pneumonia, which can result from the obstruction of the endobronchial pathway by centrally located tumors in 70% of LNET cases. Symptoms corresponding to serotonin

secretion, such as diarrhea, flushing, wheezing, carcinoid heart disease, or other hormonally active tumor products, are rarely observed (between 1%–3%). Cushing's syndrome is an even rarer condition. (14, 22, 34)

Most importantly, LCNECs are asymptomatic, and paraneoplastic syndromes are rarely seen. (35) SCLC clinical signs are mostly related to its early metastatic capabilities and local tumor growth. In approximately 10% of SCLC patients, paraneoplastic syndromes are frequently observed (30) There are endocrine types (Syndrome of Inappropriate Antidiuretic Hormone Secretion (SIADH) and Cushing syndrome), neurologic types (Subacute Cerebellar Degeneration, Lambert-Eaton myasthenic syndrome, Cancer-Associated Retinopathy), and hematologic types (anemia, leukemoid reaction, and Trousseau syndrome). (36, 37) The first positive findings usually occur on X-ray or CT imaging. The follow-up process mainly involves a PET-CT for LCNEC and SCLC and PET-CT with gallium-68 somatostatin analogues (SSAs) functional imaging for TC and AC. For further staging, an additional symptom-oriented workup should be carried out, such as an MRI for neurological symptoms. (33)

1.3. Clinical features and treatment

LNETs, specifically carcinoids, have a less aggressive nature. These lesions are typically well-differentiated and have a slow progression rate. TCs have a metastatic rate of 5-20%, while ACs can reach up to 50%. (34, 38, 39) The biological properties of these two tumors enable an effective surgical approach to their curative treatment, which is the “gold standard” in the early stages. In advanced metastatic cases, chemotherapy (ChT) and radiotherapy (RT) have little room to offer because carcinoids are generally not sensitive to these base treatments. (40) Meanwhile, LCNECs and SCLCs have a more aggressive clinical presentation; SCLC is even considered one of the most aggressive cancerous diseases. (41, 42) The key points to its invasiveness are rapid growth, early metastasis capability, and treatment resistance. (43) The initial diagnosis of these malignancies commonly reveals a high frequency of lymph node (LN) involvement (60%–80%) and distant metastases (40% in LCNEC and 60-70% in SCLC). (35) LNENs extrathoracic metastases are mostly found in the liver, brain, bone, and adrenal glands.(11, 14)

As mentioned before, the primary therapy for the early stages of these diseases is surgical resection, theoretically even for SCLC. The most frequently used technique is lobectomy

or sleeve resection; pneumonectomy should be avoided in most cases. (44) The final histological results determine its metastatic profile and LN involvement, which may indicate additional ChT or RT. Systematic nodal dissection is highly advisable and should be executed according to the national guidelines. (45, 46) Staging is acquired from the newest International Association for the Study of Lung Cancer (IASLC) 9th TNM classification. The previous version, TNM8, was used for around 7 years. (47-49) SCLC needs another staging approach. There are two categories regarding tumorous progression: limited-stage disease is localized to the ipsilateral hemithorax, whereas in the case of extensive-stage disease, the tumor has already spread beyond the ipsilateral hemithorax and includes clinical scenarios where malignant pleural or pericardial effusion or hematogenous metastases are present. (50) Patients with limited-stage disease are 30-40% of diagnoses, while extensive-stage disease is 60-70%. Regardless of the stage of SCLC, multimodality treatment is necessary with ChT and RT, and in early cases with appropriate patient selection, surgery can also be performed. (51, 52) The therapy for SCLC had no significant changes for nearly four decades. (53, 54) Cytotoxic agents are still the core of the non-surgical treatment of LNEN, typically administered in at least four cycles as part of a combination regimen using either cisplatin and etoposide or carboplatin and etoposide, or temozolomide and capecitabine.(55) (46)

RT is used in LN metastases, local control and preventing or treating brain metastases. (56)

Some patients might show symptoms associated with excessive hormone production as a paraneoplastic syndrome. Each syndrome is linked to a specific hormone: carcinoid syndrome is associated with the secretion of serotonin, Cushing's syndrome is associated with the secretion of adrenocorticotropic hormone, and acromegaly is associated with the secretion of growth hormone-releasing hormone. (57) In approximately 7-16% of SCLC cases SIADH is also observed. Its severity is directly proportional to the prognosis of these patients. (58, 59) The two most used somatostatin analogues (SSA), octreotide and lanreotide, were first admitted to surpass these syndromes, but clinical trials in advanced slowly progressive gastroenteropancreatic NE tumors showed an additional antiproliferative effect, which had a positive impact on progression-free survival (PFS) (41) The agent’s positive effect diminshed in the use of lung carcinoids (60) Everolimus showed some promising results in advanced lung NE tumors considering PFS and

pharmagological safety. (61, 62) In unresectable or metastatic cases, the guidelines recommend using SSAs as a first-line treatment for TC and slowly progressing somatostatin receptor-positive LC. For AC, everolimus is recommended as a first-line option. When we have progression after SSA treatment, we must consider everolimus for both TC and AC cases. Although modern therapy has provided a significant breakthrough in the treatment of human lung cancer in the last decade, progress in treating some of its subtypes has been slower. (63-66) Immunotherapy has limited to no indication in LNET, while showingn promising results in the treatment of SCLC. (46) Multiple clinical trials have demonstrated that immune checkpoint inhibitors, particularly when combined with chemotherapy, can significantly improve overall survival (OS) and PFS in extensive-stage SCLC. (67, 68) The use of immunotherapy for limited-stage SCLC is still not well defined, but recent wordwide data underscore the benefical role of immune checkpoint inhibitors in the management of recurrent SCLC. (69, 70)

1.4. SCLC molecular profile

SCLC has been categorized as a NE malignancy. The classic form of SCLC has unique cell morphology, strong NE marker expression, and a non-adherent growth pattern in cell cultures. (71, 72) Based on these properties, SCLC has been classified further into High-NE and Low-NE phenotypes. (73) High-NE tumors usually form irregular floating clusters, with some cells adhering *in vitro*, and their cell lines show a "classic" phenotype with small cells with unclear borders, "salt and pepper" chromatin, and small nucleoli. Low-NE tumors have loosely attached or semi-attached groups of cells, slightly larger cells with clear borders, and prominent nucleoli. In these types, there are fewer NE features and more inflammatory cells. (74, 75)

SCLC in a clinical setting is currently considered a uniform disease. Recent preclinical progress has shown different main types within an underlying molecular heterogeneity, which are inferior subtypes to the High-NE and Low-NE groups. (76) These biologically subtypes are based on the expression of transcription factors: Achaete-Scute Homologue 1 (ASCL1) SCLC-A subtype, Neurogenic differentiation factor 1 (NEUROD1) SCLC-N subtype, and POU class 2 hoemobox 3 (POU2F3) SCLC-P subtype, as well as on inflammatory characteristics (SCLC-I subtype). (77)

SCLC-A and SCLC-N are the two predominant subtypes. (78) 40-50% of SCLC cases are SCLC-A subtype with unique structural characteristics, NE profile, and l-myc oncogene (myc) amplification. Meanwhile, the SCLC-N subgroup is characterized by a low-level NE pattern, with c-myc amplification. (24, 79)

In some tumors SCLC-AN subtype is seen, where ASCL1 and NEUROD1 proteins are both highly expressed. This condition is a transitional state, which is a linear one-way process. SCLC-A is a precursor to SCLC-AN, and SCLC-AN is a precursor to SCLC-N. (24, 80-82)

Recent data suggests that SCLC-P, stands out from the previously mentioned subtypes. POU2F3 is an essential regulator in the NE-low subtypes of SCLC. POU2F3 dominant tumors and cell lines are missing typical NE markers, and instead, express tuft cell lineage markers and affect cell identity. (83) This higher expression is linked to a significantly better prognosis for recurrence-free survival. (84) Besides SCLC, basaloid squamous cell carcinoma is the only cancer type where POU2F3 expression is found. (85) SCLC-I was previously classified as an SCLC-Y subtype defined by the expression of the Yes-associated protein 1 (YAP1). Later, validation studies have failed to distinguish a unique SCLC-Y subtype in human tissue samples. These tumors can not be described by either of the previously mentioned transcription factors. We call them an immune cell (IC) - rich, inflamed phenotype. (11)

SCLC subtype landscape is complex with high tumor plasticity and heterogeneity. A predominant subtype does not necessarily define the whole tumor. The cells either express specific markers for their subtype or have a silent phenotype. These cells can be mixed or found in separate nests within the tumor. (11, 54, 76) According to this behaviour, a recent study explored the NE phenotypes of primary SCLC and their corresponding LN metastases, revealing significant intertumoral heterogeneity. Through cluster analysis, distinct High-NE and Low-NE subtypes were clearly delineated, and in some cases notable changes in NE characteristics were observed between primary and LN metastatic lesions. These results show the complexity of SCLC and indicate that the NE profile of LN metastases may not fully represent the primary tumors' (PT) properties, which can misguide diagnosis and treatment. (86)

2. Objectives

In our first study, we investigated the spatial heterogeneity of SCLC between PTs and corresponding LN metastases, whereas our second study aimed to assess the key differences in the immunological profiles of LNENs (SCLC, LCNEC and AC).

2.1. Investigating Inter-tumoral Heterogeneity in SCLC

Our objective was to explore the inter-tumoral heterogeneity between SCLC PTs and their corresponding LN metastases using surgically resected representative tissue samples. Following the pathological preparations, we analyzed RNA-Seq and IHC data to identify unique molecular and cellular characteristics. Additional statistical tests were used to compare the differences between the PTs and matched LNs metastases. This research should provide insights into the extent of inter-tumoral heterogeneity and tumor plasticity in SCLC. The study was conducted by the Helsinki Declaration of the World Medical Association and received approval from the Hungarian Scientific and Research Ethics Committee of the Medical Research Council (ETT-TUKEB-7214-1/2016/EKU).

2.2. Analysis of Immunophenotypic Differences in Neuroendocrine Lung Neoplasm

Our second study focused on intermediate-grade (AC) and high-grade (SCLC and LCNEC) NE lung cancers and their immunophenotypic differences, using IHC methods. The cohort involved four European centers. Statistical tests were used to assess differences in the expression levels of immune markers. The study was approved by the national-level ethics committee of Hungary, by the Hungarian Scientific and Research Ethics Committee of the Medical Research Council (ETT TUKEB 39249–2/2019/EKU and 52614–4/). Our findings may have diagnostic significance for these highly aggressive tumor types and could aid in designing and implementing novel immunotherapeutic clinical trials.

3. Methods

3.1. Investigating Inter-tumoral Heterogeneity in SCLC

3.1.1. Study population and treatment

This study involved 32 patients with SCLC who had LN metastasis and underwent surgical resection between 1978 and 2013 at the National Korányi Institute of Pulmonology in Budapest, Hungary. PTs and their corresponding LN metastases were collected during surgery. We retrospectively retrieved clinicopathological data, including gender, age at the time of surgery, smoking history, surgical parameters, and survival data from medical records and the Central Statistical Office of Hungary. All identifying information was removed after clinical data collection, making it impossible to directly or indirectly identify patients. Due to the study's retrospective design, the requirement for individual informed consent was waived.

The therapeutic strategies were implemented following the current National Comprehensive Cancer Network (NCCN) guidelines. Surgical procedures included anatomic resections, such as lobectomy or pneumonectomy, and wedge resections. When indicated, adjuvant ChT was administered using either a platinum-etoposide doublet regimen or a combination of cyclophosphamide, epirubicin, and vincristine. Notably, none of the patients in this study received immunotherapy.

3.1.2. Ribonucleic acid (RNA) expression analysis

FFPE tissue samples from PTs and corresponding LNs metastases were macrodissected for molecular analysis. RNA expression profiling was conducted using the HTG EdgeSeq Targeted Oncology Biomarker Panel (HTG Molecular Diagnostics Inc., Tucson, AZ, USA), enabling simultaneous and quantitative detection of 2,560 genes associated with tumor biology. This targeted RNA expression assay employs a nuclease protection method involving the hybridization of target RNA to a complementary deoxyribonucleic acid probe followed by single-strand nuclease treatment. The panel was specifically designed to identify well-established cancer-specific therapeutic targets and markers of drug response. Assay validation was performed using appropriate positive and negative controls.

3.1.3. Tissue processing and IHC

Before enrolment, all hematoxylin and eosin (H&E)-stained slides were re-evaluated by a board-certified pulmonary pathologist to confirm the diagnosis of SCLC. Quality control of older blocks was achieved within our previous study framework by performing confirmatory IHC staining with routinely used diagnostic antibodies. (81) Tissue microarray (TMA) construction was performed at the University of Colorado, Denver (Aurora, CO, USA), as previously described. (87) Notably, two 1-mm tissue punches were taken from each donor tissue block and placed into a recipient paraffin block in a positionally encoded array format (MP10 1.0-mm tissue punch on a manual TMA instrument, Beecher Instruments). Tissue cores were retrieved from the most viable tumor areas defined on H&E-stained slides. In addition to subtype markers (ASCL1, NEUROD1, POU2F3, and YAP1), the expression of the following clinically relevant proteins were also evaluated: CD47, c-myc, l-myc, delta-like ligand 3 (DLL3), enhancer of zest homolog 2 (EZH2), lysine-specific demethylase 1 (LSD1), mammalian target of rapamycin proteins (mTOR), PD-L1, and phosphoinositide 3-kinase (PIK3). Concerning IHC staining, after deparaffinization and rehydration of the four μm-thick sections, slides were heated for 20 minutes in either 10 mM citrate buffer (pH 6.0) or 10 mM Tris-EDTA buffer (pH 9.0) according to antibody protocols. Slides were incubated in a 0.3% hydrogen peroxide (H_2O_2) solution to reduce background staining. Signal amplification was performed according to the manufacturer's recommendation of the Novolink TM Polymer Detection System kit from Leica Biosystems (RE7150-K; Wetzlar, Germany), followed by antibody incubation at room temperature for one hour. The used antibodies are listed in Table 1. Antibody binding was detected with the ImmPACT 3-3′-diaminobenzidine (DAB) substrate Kit from Vector Laboratories (NC9567138; Newark, CA, USA). Nuclei were counterstained using hematoxylin. All antibodies were validated with appropriate tissue controls. IHC-labeled and H&E-stained slides were digitally scanned using PANNORAMIC 250 Flash III (3DHISTECH Ltd., Budapest, Hungary); sections were evaluated with CaseViewer 2.4 (3DHISTECH Ltd., Budapest, Hungary). The expression level of the given marker was examined blinded to clinical data by two experienced independent pathologists, and the staining index (percentage of TCs showing positive staining reported to all TCs) was determined.

Table 1. Antibodies used for IHC.

	COMPANY	CATALOG NR.	HOST		ANTIGEN RETRIEVAL
ASCL1	BD Pharmigen; Berkshire, UK	556604	Mouse	1:50	Citrate (pH=6.0)
NEUROD1	Abcam; Boston, MA, USA	ab213725	Rabbit	1:100	Tris-EDTA (pH=9.0)
POU2F3	Santa Cruz Biotechnology; Dallas, TX, USA	cs-293402	Mouse	1:100	Citrate (pH=6.0)
YAP1	Cell Signaling Technology; Leiden, The Netherlands	49125	Rabbit	1:200	Citrate (pH=6.0)
EZH2	Cell Signaling Technology; Leiden, The Netherlands	5246S	Rabbit	1:50	Citrate (pH=6.0)
DLL3	Abcam; Boston, MA, USA	ab103102	Rabbit	1:100	Tris-EDTA (pH=9.0)
PIK3CA	Bioss; Woburn, MA, USA	bs-2067R	Rabbit	1:400	Citrate (pH=6.0)
MTOR	Abcam; Boston, MA, USA	ab32028	Rabbit	1:400	Citrate (pH=6.0)
LSD1	Abcam; Boston, MA, USA	ab17721	Rabbit	1:200	Tris-EDTA (pH=9.0)
TIGIT	Abcam; Boston, MA, USA	ab243903	Rabbit	1:100	Tris-EDTA (pH=9.0)
CD47	Sigma-Aldrich; St. Louis, MI, USA	HPA044659	Rabbit	1:100	Tris-EDTA (pH=9.0)
PD-L1	Abcam; Boston, MA, USA	ab205921	Rabbit	1:500	Citrate (pH=6.0)

C-MYC	Abcam; Boston, MA, USA	ab32072	Rabbit	1:100	Tris-EDTA (pH=9.0)
L-MYC	Thermo Fisher Scientific; Waltham, MA, USA	PA5-41114	Rabbit	1:200	Tris-EDTA (pH=9.0)
BCL-2	Leica Biosystems; Wetzlar, Germany	PA0117	Mouse	1:100	Tris-EDTA (pH=9.0)

3.1.4. Statistical analysis

RNAseq data was quantified as "normalized counts per million (CPM)," measuring the number of sequenced fragments aligning to a specific gene out of 1 million sequenced reads, normalized with the length of the gene. The initial analysis of RNAseq results was performed automatically by the default processing pipeline utilized by the HTG EdgeSeq Targeted Oncology Biomarker Panel. Subsequent investigations were based on the resulting normalized CPM values. Fold-changes (FC) between the expression levels of LN metastases and PTs were calculated by dividing the expression (normalized CPM or IHC positivity) of the given gene/protein in the LN sample by the expression level of the same gene/protein in the PT sample of the same patient. The log2-transforms of these ratios are shown in the figures. Expression levels across different sample origins (PTs and LNs metastases) were compared with t-tests and Wilcoxon signed-rank tests. Correction for multiple testing was performed using the Holm method. Correlations between expression levels measured with the two experimental protocols (IHC staining vs. RNAseq) were assessed by calculating the Pearson correlation coefficients and the corresponding p-values. Hierarchical clustering of samples based on expression levels was performed with the Complex Heatmap R package (version 2.10.0). The distance matrix was calculated using Euclidean distance measures, and the dendrograms were created using the ward D clustering method. To determine whether PTs and LN metastases are linearly separable in the expression space of the genes and proteins of interest, principal component analysis (PCA) was performed with the facto extra R package (version 1.0.7). Before PCA, expression levels were centered and scaled to have zero mean and unit variance. All statistical analyses were performed in R version 4.2.1 (R Foundation for Statistical Computing, Vienna, Austria).

3.2. Analysis of Immunophenotypic Differences in Neuroendocrine Lung Neoplasm

3.2.1. Study population and treatment

The primary study was divided into two cycles, NE1 and NE2 study.

The first stage (NE1) was a two-center retrospective study, which included 85 Caucasian patients with histologically confirmed LNENs. These patients had a surgical resection at either the National Korányi Institute of Pulmonology or the National Institute of Oncology in Budapest, Hungary, between 2000 and 2020. Among these patients, 26 were diagnosed with AC, 30 LCNEC, and 29 SCLC. Clinical and pathological data, including age at diagnosis, gender, comorbidities, and smoking history, were collected retrospectively from medical records. Survival outcomes were obtained from the National Health Insurance Office and the Central Statistical Office of Hungary. Only patients with comprehensive clinicopathological data and sufficient FFPE tumor tissue were included. Additionally, 10 TC samples were incorporated into the study for comparative analysis with AC samples. The requirement for individual informed consent was waived due to the study's retrospective nature. Patient identifiers were removed after data collection to prevent direct or indirect identification. All patients underwent lung resection surgery, including lobectomy or wedge resection, and platinum-based adjuvant ChT was administered when necessary. Systemic therapy followed the current NCCN guidelines in both institutions.

3.2.2. IHC

Tumor tissue samples were obtained through surgical resection and examined by a board-certified pathologist using routine diagnostic protocols and IHC staining for markers such as Chromogranin A, Synaptophysin, CD56, Syntaxin, and Ki-67. To ensure diagnostic accuracy and exclude mixed histology cases, all H&E-stained slides were independently reviewed before inclusion. Tissue sections were analyzed for 15 immunological markers (PD-L1, PD-1, CD3, CD4, CD8, CD27, CD47, Indolamine 2,3-dioxygenase (IDO), inducible T-cell costimulator (ICOS), CD70, CD137, CD40, CD94/NK Group 2 Member A (NKG2A), lymphocyte-activation gene 3 (LAG3), and tumor necrosis factor receptor superfamily, member 4 (OX40), which are potential immunotherapy targets. (88-92)

After deparaffinization and rehydration, tissue sections were treated with a 3% H_2O_2 solution for 20 minutes to minimize nonspecific background staining. Following this,

samples were heated to 98°C in a 10 mM Citrate buffer (pH 6.0) or a 10 mM Tris-EDTA buffer (pH 9.0) for 40 minutes, according to the manufacturer's guidelines. The slides were then incubated at room temperature with Ultra V Block (Ultravision LP detection system, Lab Vision Corporation, Thermo Fisher Scientific Inc., Pittsburgh, MA, USA) for 5 minutes, followed by overnight incubation with primary antibodies at 4°C. Immunoreactions were visualized using the UltraVision LP detection system and stained with DAB, followed by hematoxylin counterstaining. The slides were digitally scanned using the PANNORAMIC 250 Flash III system (3DHISTECH Ltd., Budapest, Hungary) and analyzed using CaseViewer 2.4 software (3DHISTECH Ltd., Budapest, Hungary).
Pathological evaluation was performed by averaging the percentage of positive cells across ten randomly selected areas, assessed independently by two pathologists at 20x and 40x magnification. A third senior lung pathologist reviewed the slides to see if the scores differed by more than 20%. Separate scoring was conducted for tumors and ICs, with the proportion of positive cells calculated relative to the total tumor and IC populations, including the overall immune infiltrates in each sample.

Manual analysis was chosen over computational methods because the antibodies studied are not yet commonly used in clinical diagnostics, and existing software is primarily designed for standard diagnostic antibodies. Furthermore, the study lacked the extensive datasets needed to train AI-based algorithms effectively.

3.2.3. Statistical analysis

Statistical analyses were performed using R version 4.0.5 (R Foundation for Statistical Computing, Vienna, Austria). P-values of < 0.05 were considered statistically significant. The Bonferroni correction was applied in some instances to compensate for multiple tests.

4. Results

4.1. Investigating Inter-tumoral Heterogeneity in SCLC

4.1.1. Patient and sample characteristics

The study included 32 surgically treated patients with histologically confirmed SCLC. The median age of the patients was 58 years (range: 34–78), with 22 male participants. All patients were of Caucasian descent. The median OS was 20.7 months, while the median disease-free survival was 14.9 months.

4.1.2. Comparative expression analysis of molecules of interest

Figure 1 provides an overview of RNAseq data highlighting differences in gene expression between PTs and corresponding LN metastases. After correcting for multiple testing and applying a log2 fold change (log2-FC < 0) threshold, the five most significantly downregulated genes in LN metastases compared to PTs were PGC, FIGF, ROS1, CFTR, and TMPRSS2. Notably, the molecules of interest for this study showed no significant differences in RNA expression levels between PTs and LN metastases (Figure 2A and Figure 1). Protein-level expression patterns were subsequently evaluated using IHC. As shown in Figure 2B, DLL3 expression was significantly higher in PTs than in LN metastases ($p = 0.008$). Similarly, the mean expression levels of CD47, LSD1, mTOR, and POU2F3 were higher in PTs, though these differences were not statistically significant. Conversely, NEUROD1 expression was significantly lower in PTs compared to LN metastases ($p < 0.001$), while c-myc expression showed a non-significant reduction in PTs. Representative IHC images illustrating the expression of each marker in PTs and LN metastases are provided in Figure 3.

DOI:10.14753/SE.2025.3289

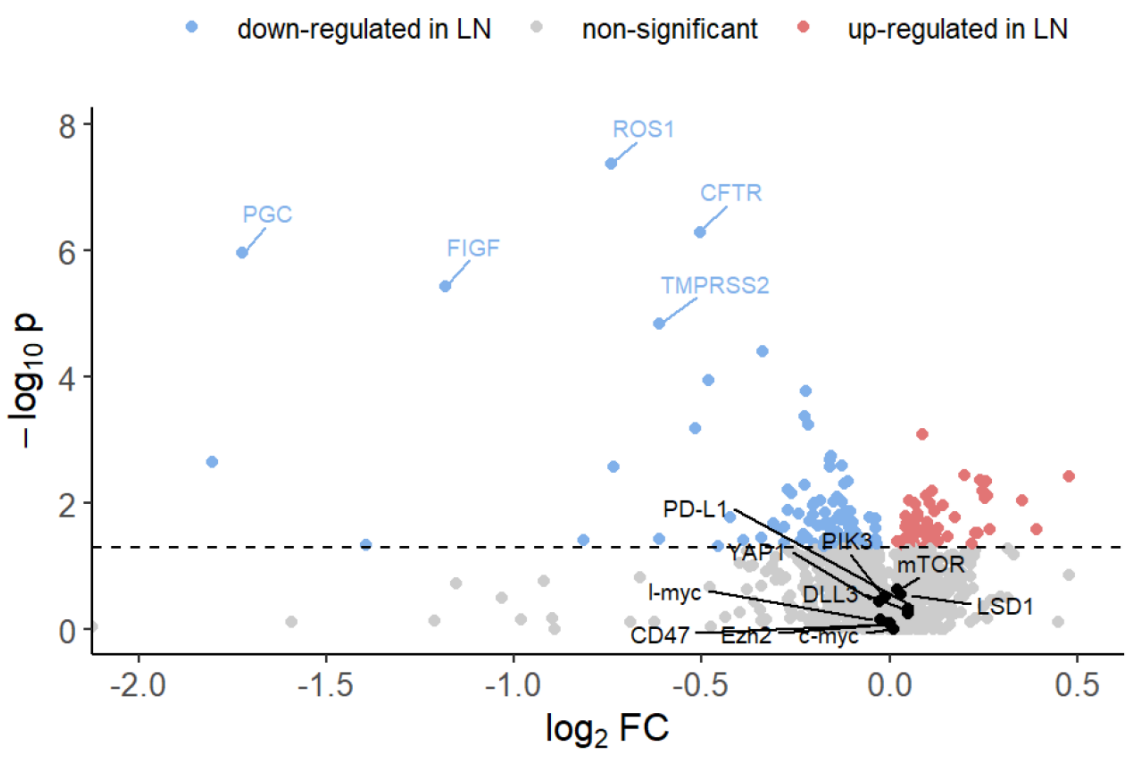

Figure 1. Volcano plot of gene expression differences between PTs and LN metastases. Each dot represents a single gene. Non-significantly differentially expressed genes are represented with grey dots. Genes of interest are labeled black. Genes with significant differential expressions after correction for multiple testing are labeled with blue (down-regulated in LNs) or red (up-regulated in LNs).

DOI:10.14753/SE.2025.3289

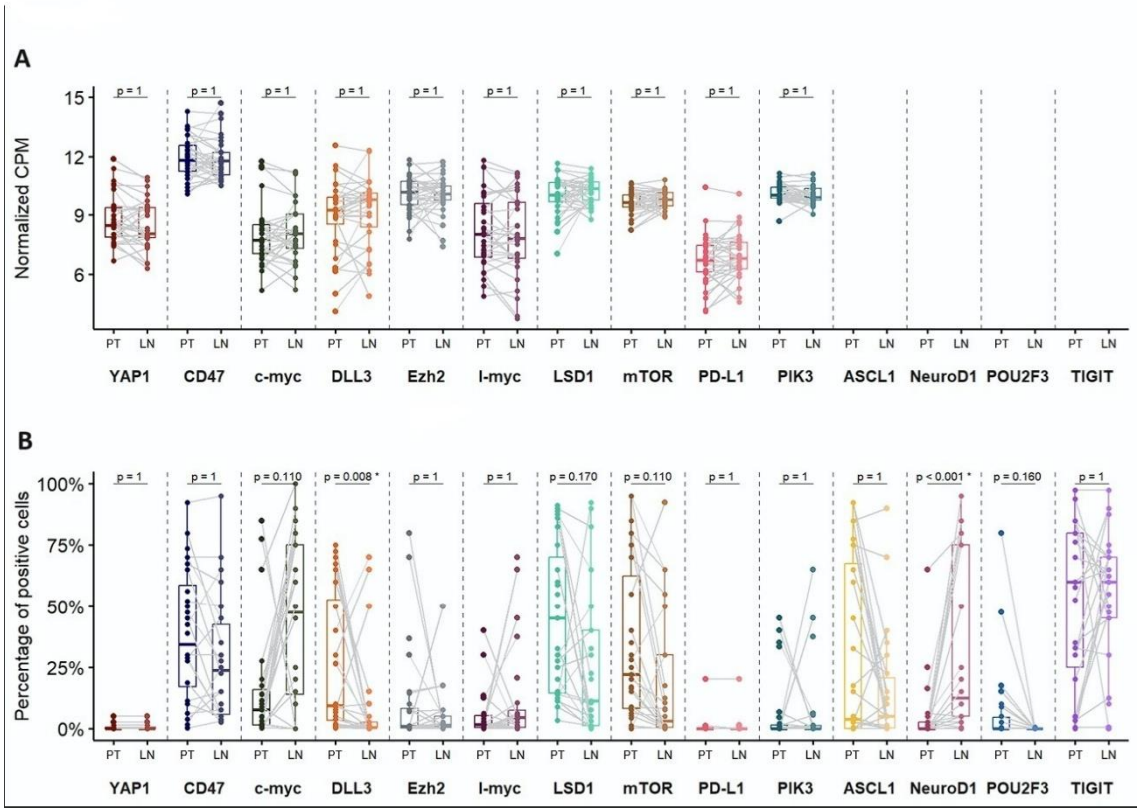

Figure 2. Expression pattern of genes (A) and proteins (B) of interest in SCLC primary tumors (PTs) and lymph node (LN) metastases. The p-values were calculated using t-tests (A) and paired Wilcoxon signed-rank tests (B). For multiple correction testing, the Holm method was applied. DLL3 expression was significantly higher in the PTs than in the LN metastases, whereas NEUROD1 expression was substantially lower in the primary lesions (vs. LN metastases). Results significant after correction are marked with an asterisk (*).

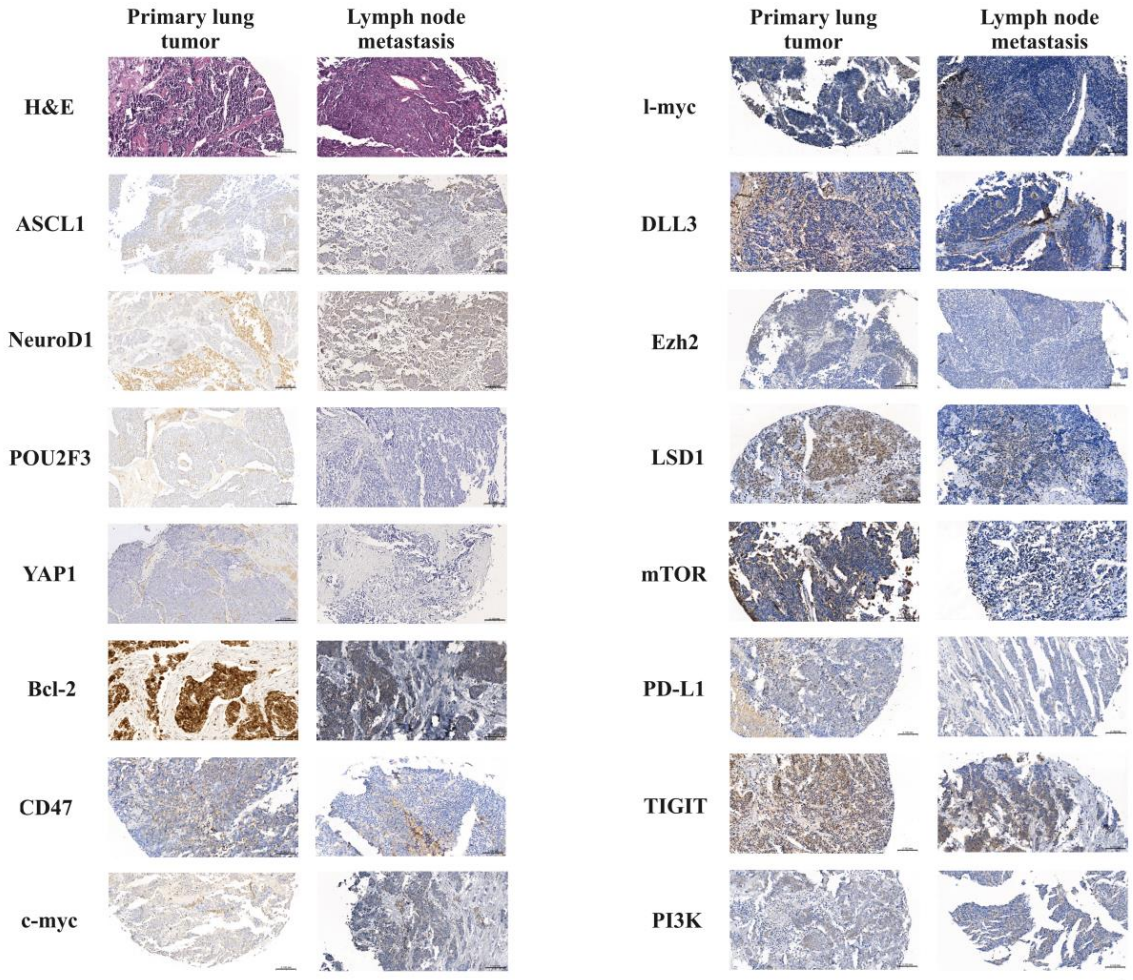

Figure 3. IHC stainings of FFPE primary and LN metastatic SCLC samples with subtype markers and other proteins of interest. The representative images were captured with a 20x objective lens. The positive cells were visualized with DAB, and the nuclei were labeled with hematoxylin. The top left row corresponds to the routine H&E-staining.

4.1.3. Correlation between expression levels as defined by RNA expression analysis and IHC

A moderate to weak correlation was observed between RNA expression data and IHC results. No correlation was found for the expression of YAP1, c-myc, DLL3, EZH2, l-myc, LSD1, mTOR, and PIK3 across the two datasets. However, a moderate positive correlation was identified for CD47 ($R = 0.316$; $p = 0.020$) and PD-L1 ($R = 0.585$; $p < 0.001$) expression, as illustrated in Figure 4.

DOI:10.14753/SE.2025.3289

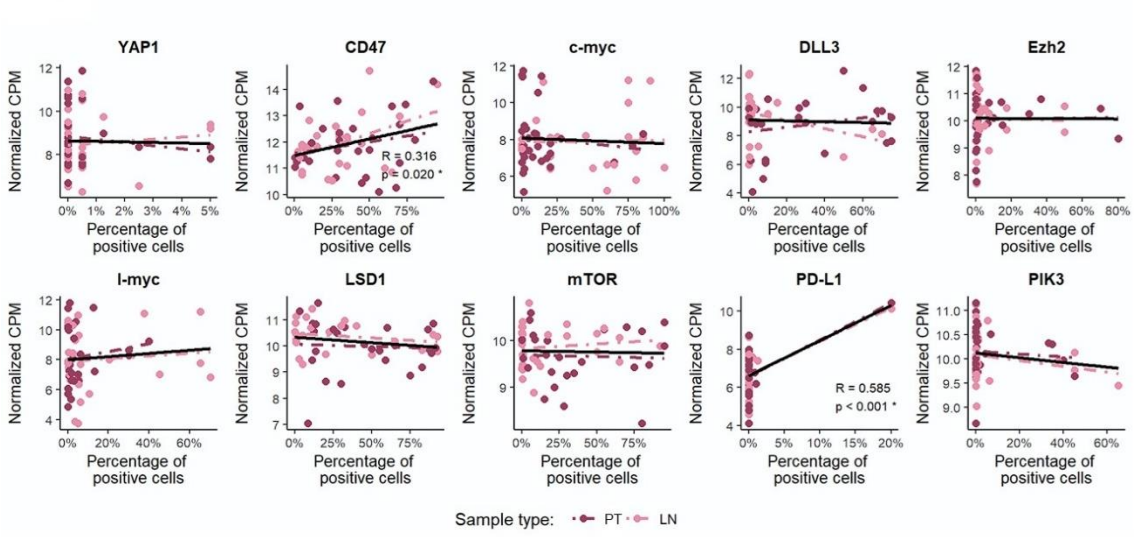

Figure 4. Protein and gene expression data correlate as defined by IHC and RNA expression analysis. Colors indicate sample type (PT: primary tumor, LN: lymph node metastasis). R indicates the Pearson correlation coefficient, and p shows the corresponding p-value. Statistically significant results are marked with an asterisk (*).

4.1.4. Hierarchical clustering and PCA of expression levels

Next, we explored whether protein expression patterns could differentiate between PTs and LN metastases. As shown in Figure 5A, while cluster analysis identified two distinct subgroups with differing protein expression profiles, these clusters did not align with the site of origin. Notably, the transcription factor YAP1 consistently exhibited low expression levels across all sample types. In contrast, TIGIT, an immune checkpoint involved in immune suppression, was overexpressed in most primary and LN metastatic tumors. Interestingly, mTOR and DLL3, emerging as potential therapeutic targets in SCLC, showed variable expression levels among tumors. PD-L1 expression was generally low, with few exceptions.

PCA (Figure 5B) revealed that the first three principal components accounted for 47.4% of the variance in the data. Only a modest separation between PTs and LN metastases was observed when projecting the samples onto the space defined by the first two principal components. This suggests that protein expression levels, as determined by IHC, cannot

DOI:10.14753/SE.2025.3289

reliably distinguish between samples of different origins. Similarly, RNA expression data failed to classify samples based on their site of origin (Figure 6).

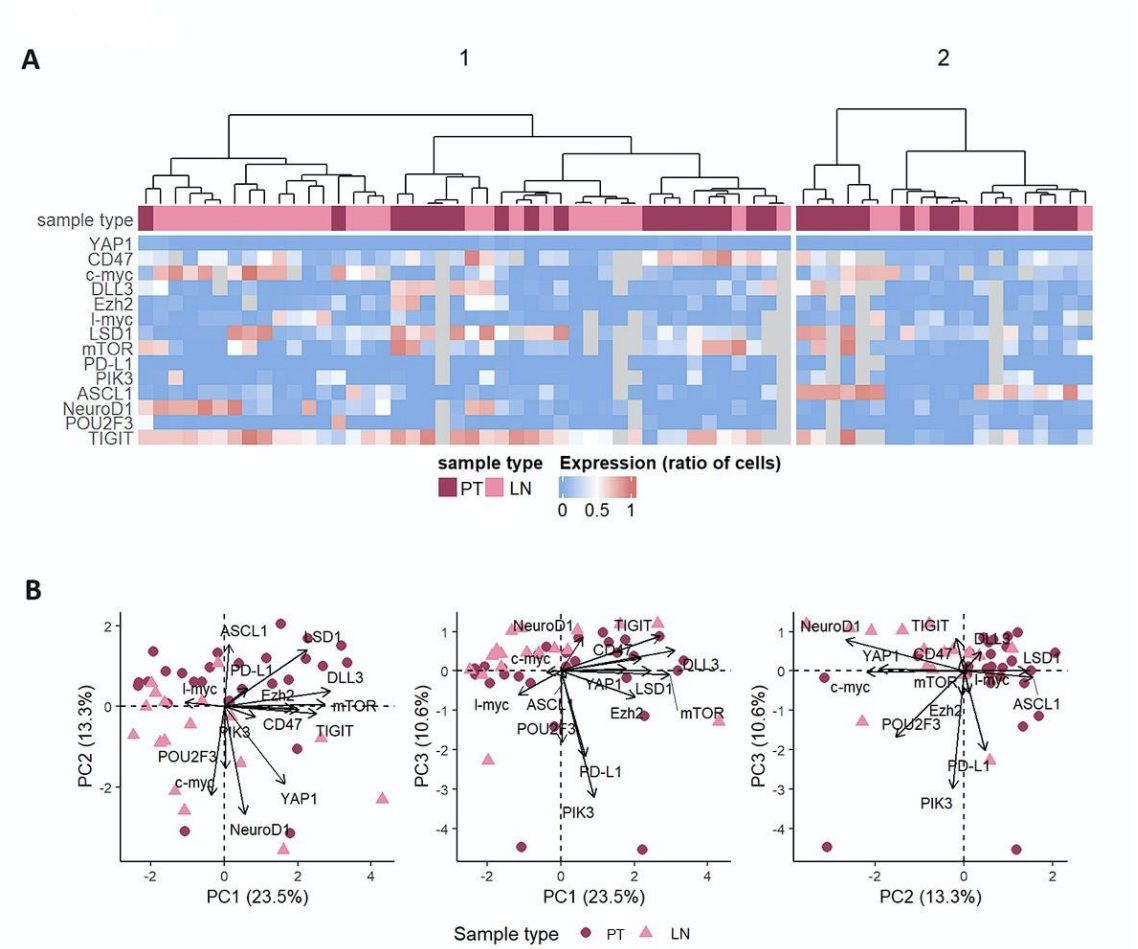

Figure 5. Hierarchical clustering (A) and principal component (PC) analysis (B) of primary tumors (PTs) and lymph node (LN) metastases based on the tumor cell expression of proteins of interest. (A) The color of the bars on the top of the heatmap indicates the sample type. Heatmap colors correspond to IHC staining positivity, defined as the ratio of positive cells. The hierarchical clustering of samples cannot effectively differentiate between PTs and LN metastases based on the expression pattern of proteins of interest. (B) The panels show the samples projected to the subspaces the first three PCs spanned. Colors indicate sample type. The percentage of variance each PC explains is displayed in the axis labels. Arrows indicate the direction of the protein expression levels in the subspaces. IHC expression levels of the investigated proteins alone cannot distinguish between samples of different origins.

DOI:10.14753/SE.2025.3289

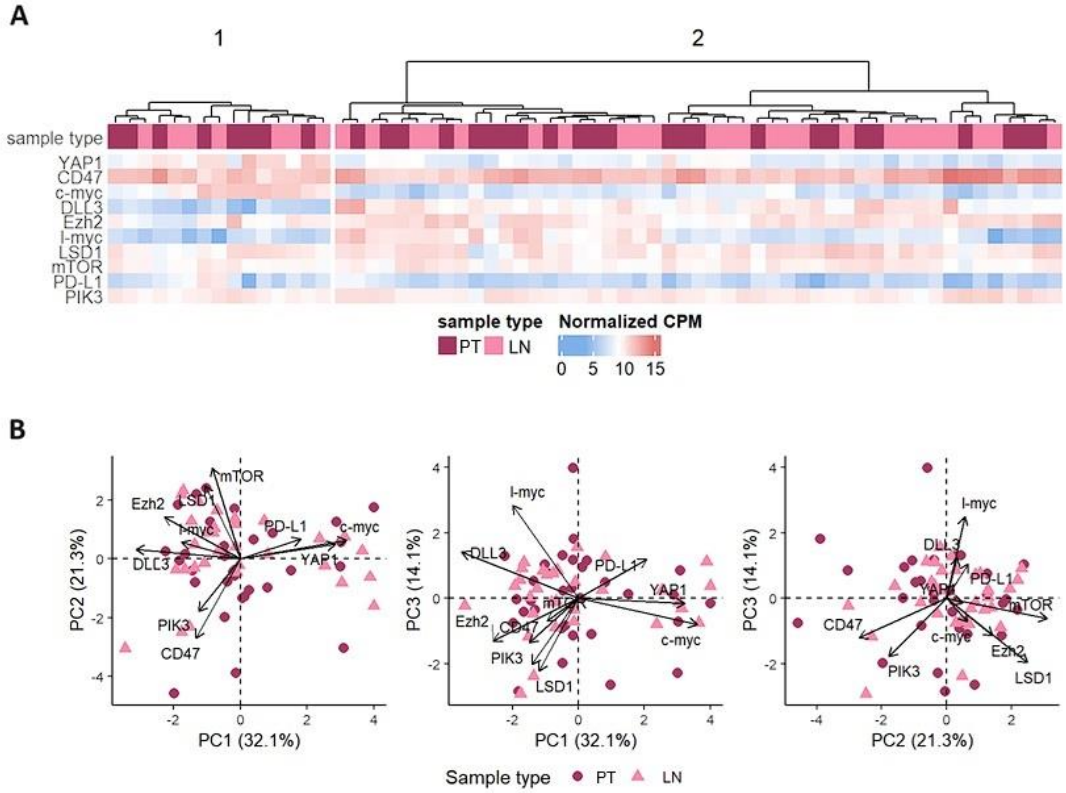

Figure 6. Hierarchical clustering (A) and principal component (PC) analysis (B) of primary tumors (PTs) and lymph node (LN) metastases based on RNA expression of molecules of interest. Using the RNA expression data of YAP1, CD47, c- myc, DLL3, EZH2, l-myc, LSD1, mTOR, PD-L1, and PIK3 samples could not be classified according to their site of origin.

4.1.5. Comparative IHC analysis reveals molecular subtype change between PTs and corresponding LN metastases.

Differential expression analysis of subtype-defining proteins identified five major SCLC subgroups across the tumor samples. As shown in Figure 7, these subgroups included SCLC-A, SCLC-AN, SCLC-N, SCLC-P, and the previously proposed quadruple-negative SCLC subtype (SCLC-QN), which was characterized by low expression of all four transcriptional regulators (ASCL1, NEUROD1, POU2F3, and YAP1). However, no distinct YAP1-defined subtype was identified through cluster analysis. Most samples (61%) exhibited a NE phenotype, encompassing the SCLC-A, SCLC-AN, and SCLC-N subgroups. Next, we investigated whether the subtype of PTs matched that of their corresponding LN metastases or if there were notable differences in subtype-defining

protein expression. The analysis revealed that LN metastases often differed from their PT counterparts, with primary and metastatic lesions frequently clustering into different subgroups (Figures 7 and 8). Molecular subtype changes were observed in 21 cases. Most commonly, SCLC-QN PT transitioned to SCLC-AN (n=5) or SCLC-N (n=5) in their LN metastases. Other changes included transitions from SCLC-A to SCLC-AN (n=4), SCLC-N (n=1), or SCLC-QN (n=3). Interestingly, the majority of SCLC-AN PTs retained their subtype during metastatic spread, with only one case switching to SCLC-N. Notably, none of the PTs exhibited an SCLC-N subtype, yet it was the second most common subtype in LN metastases. Both SCLC-P PTs transitioned to SCLC-N in their LN metastases.

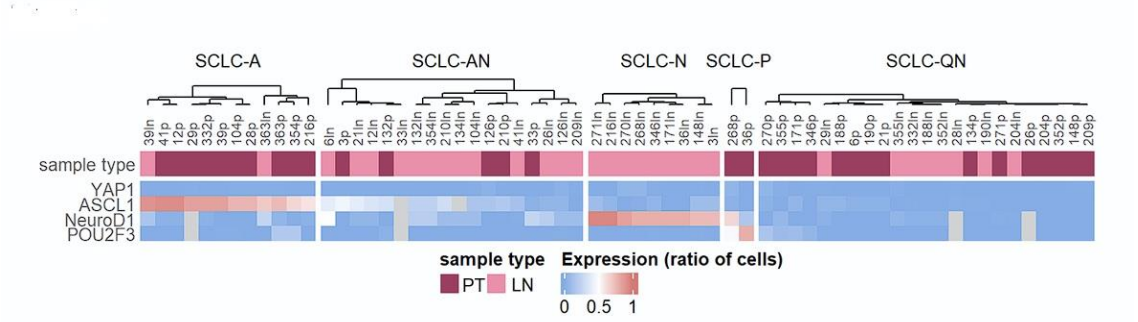

Figure 7. Molecular subtypes of surgically resected PTs and LN metastases as defined by IHC. Hierarchical clustering of primary tumors (PTs) and lymph node (LN) metastases revealed five distinct SCLC subgroups: SCLC-A, SCLC-N, SCLC-AN, SCLC-P and SCLC-QN. The color of the bars on the top of the heatmap indicates the sample type. Heatmap colors correspond to IHC staining positivity, which is defined as the ratio of TCs showing positive staining. PTs and their corresponding LN metastases frequently cluster in different subgroups.

DOI:10.14753/SE.2025.3289

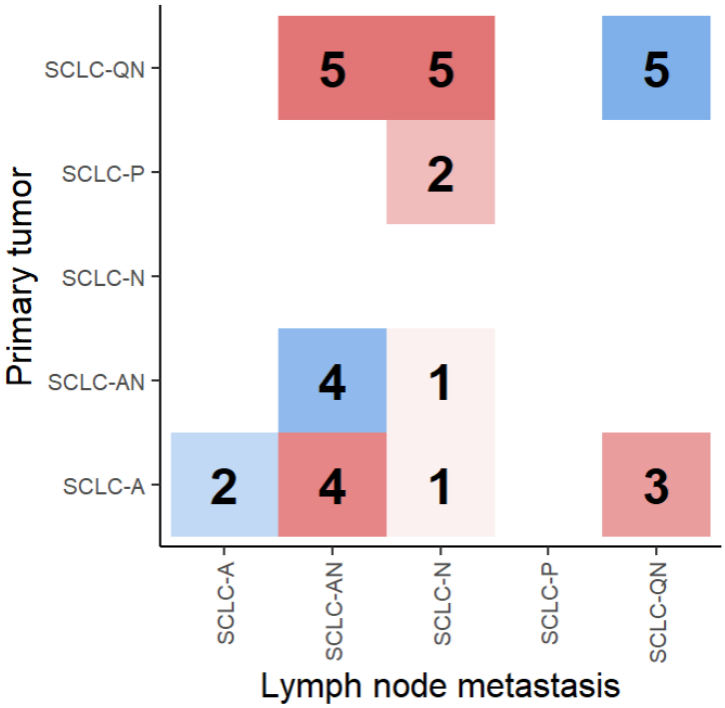

Figure 8. Molecular subtypes of SCLC PTs and their corresponding LN metastases. Blue cells indicate no subtype change between the two samples of different origins (y-axis: primary tumor, x-axis: LN metastasis), while red marks a change in the molecular subtype. The number of patients affected and not affected by subtype change is shown in the corresponding cells. The most common changes include SCLC-A to either SCLC-AN or SCLC-QN, and SCLC-QN to either SCLC-AN or SCLC-N. Interestingly, SCLC-AN PTs tended to have the same subtype in their LN metastasis. None of the LN metastases had SCLC-P subtype, despite two SCLC-P PT.

4.2. Analysis of Immunophenotypic Differences in Neuroendocrine Lung Neoplasm

4.2.1 Clinicopathological characteristics and survival outcomes of included patients

Patient characteristics categorized by their tumor's histological type are detailed in Figure 9A. Notably, PTs location was precisely determined based on bronchoscopic visualization, as bronchoscopy reports were available for all patients. Regarding the relationship between clinicopathological factors and survival outcomes, our univariate analysis revealed that lung cancer subtype (log-rank p = 0.059), vascular involvement

DOI:10.14753/SE.2025.3289

(log-rank p = 0.0049), and diabetes as a comorbidity (log-rank p = 0.021) significantly impacted overall survival (OS) (Figure 9B).

A

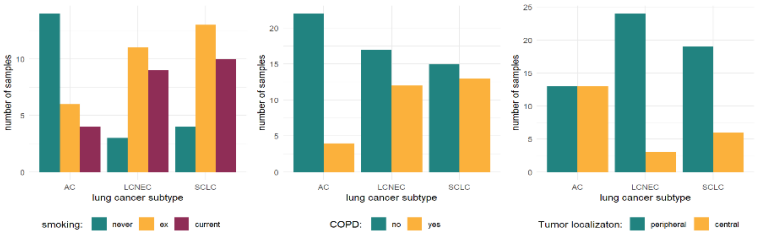

B

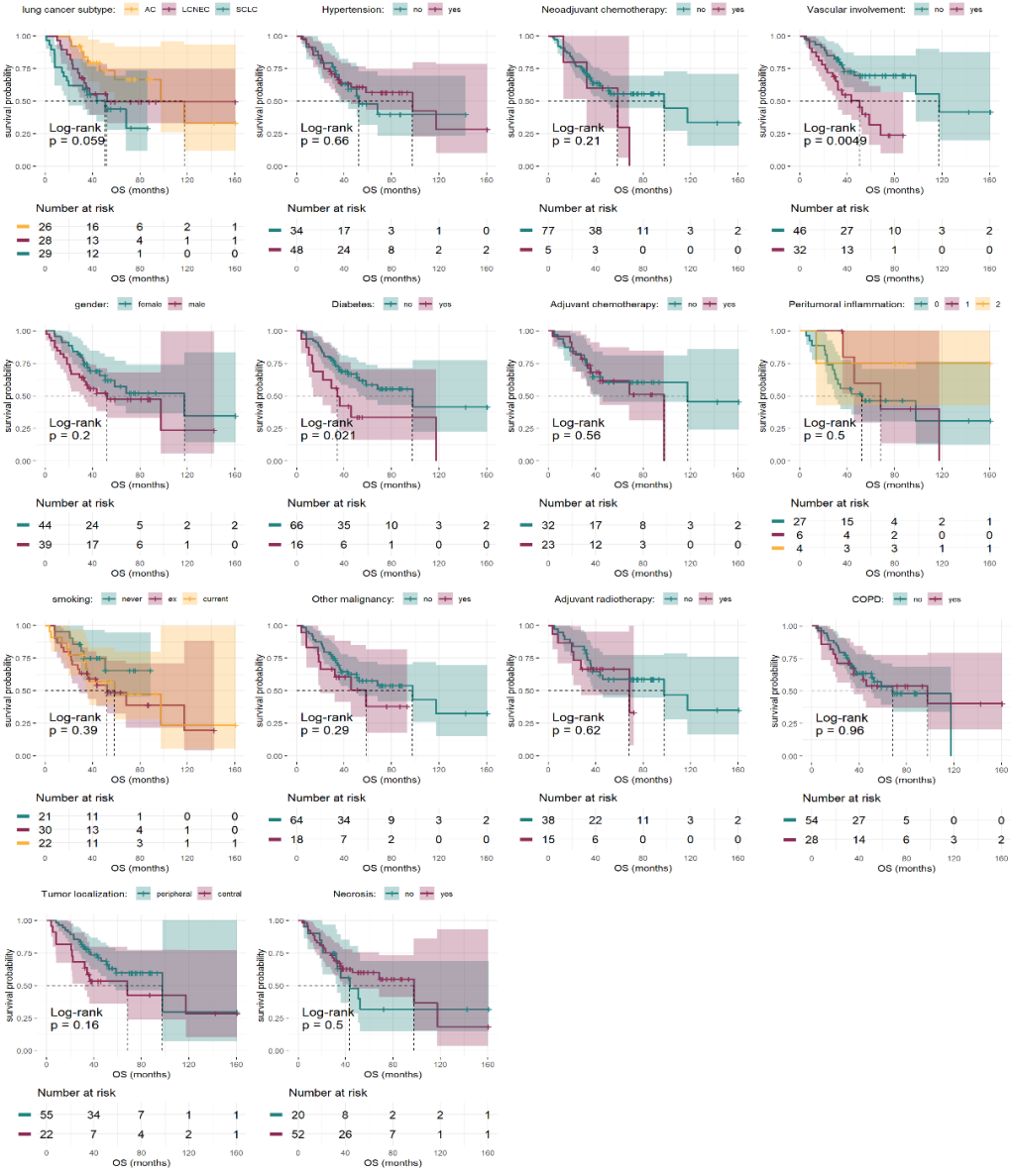

Figure 9. (A) Relevant associations between histological types and clinical parameters. The horizontal axis shows the investigated clinical variables, whereas the number of samples is displayed on the vertical axis. AC tumors occur more frequently in never smokers (vs. former or current smokers) and in non-COPD patients. LCNEC and SCLC tumors tend to be peripherally located and have higher tumor grades than ACs (this latter association remained statistically significant even after multiple testing corrections). **(B) Kaplan-Meier survival estimates according to clinicopathological parameters.** SCLC tumor type, vascular involvement, high histological grade, and the presence of diabetes were associated with impaired OS. AC, atypical carcinoid; LCNEC, large cell neuroendocrine carcinoma; COPD, chronic obstructive pulmonary disease; SCLC, small-cell lung cancer; OS, overall survival.

4.2.2 The impact of tumor immune microenvironment (TIM) on survival outcomes in LNEN patients

Patients were categorized into low- and high-expression groups for each immune-related marker using the median value as the cutoff. Univariate Kaplan-Meier survival analysis indicated a trend toward worse OS in patients with high CD47-expressing tumors compared to those with low expression (log-rank p = 0.096). Conversely, high tumor cell CD40 expression was linked to better survival outcomes (log-rank p = 0.052; Figure 10A). For immune-related markers in ICs, high CD137 expression was significantly associated with improved OS (log-rank p = 0.0096, Fig. 4B). In contrast, high IC ICOS expression was associated with poorer survival outcomes (log-rank p = 0.045, Figure 10B). Borderline significance was observed for IC-based expression of CD8 and LAG3 concerning OS (Figure 10B), with high CD8 expression showing a trend toward worse OS (p = 0.083) and high LAG3 expression suggesting a trend toward improved OS (p = 0.15). When analyzing SCLC and LCNEC samples separately, none of the tumor cell marker expressions significantly affected OS in the univariate analysis (Figure 11A). However, in ICs, significant survival differences were observed for PD-1 (p = 0.048), CD27 (p = 0.0043), LAG3 (p = 0.023), CD4 (p = 0.059), CD137 (p = 0.064), and the extent of immune infiltration (p = 0.021) (Figure 11B).

DOI:10.14753/SE.2025.3289

A

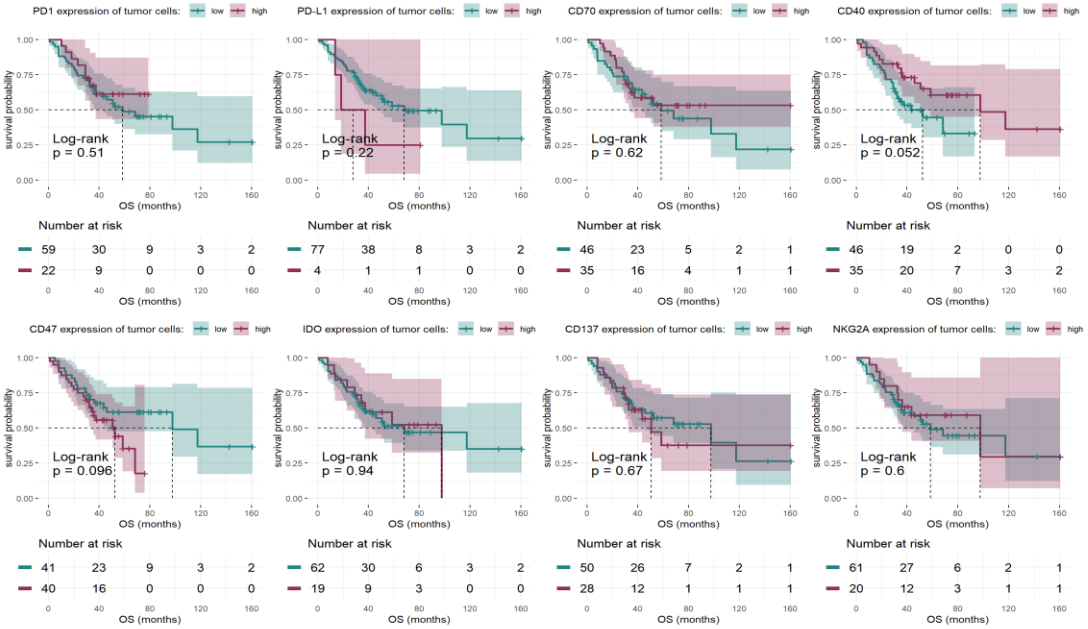

B

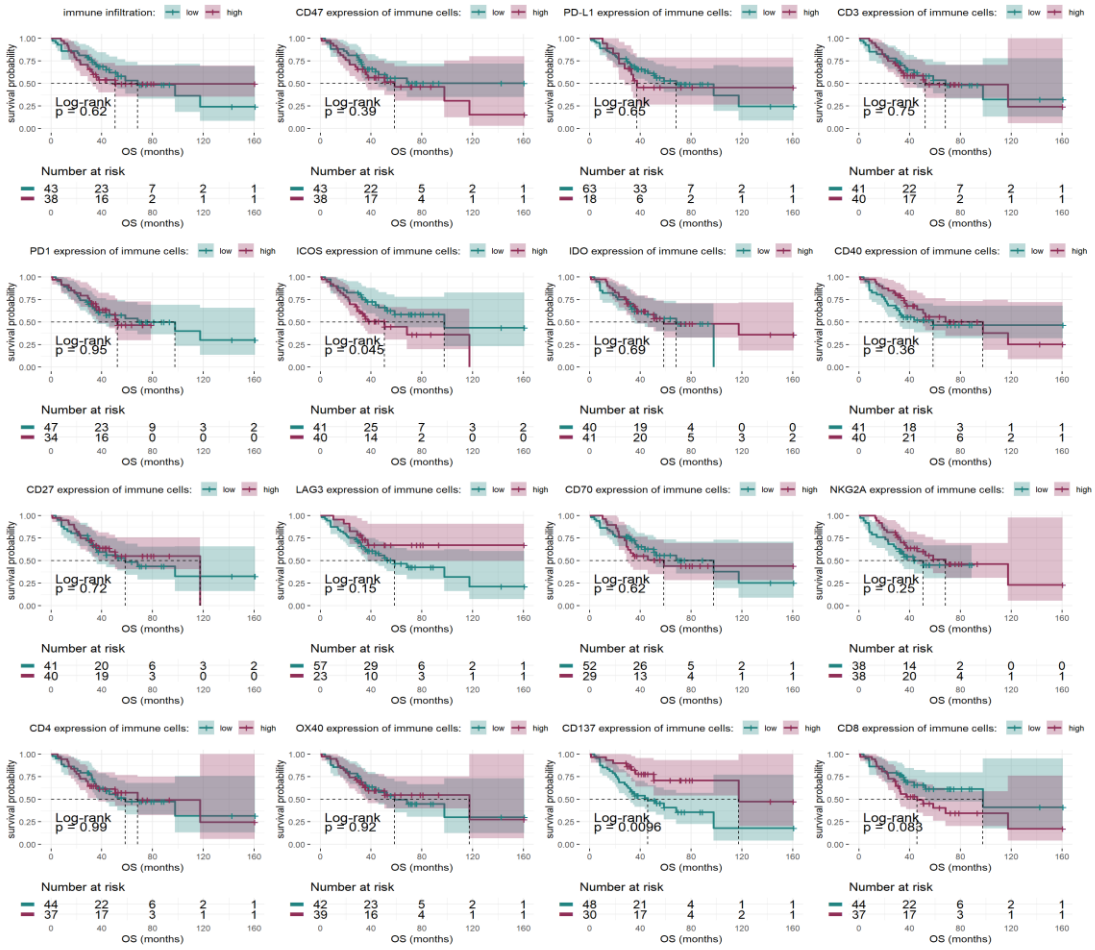

DOI:10.14753/SE.2025.3289

Figure. 10. Kaplan-Meier estimates for OS concerning the expression pattern of immune-related markers by TCs (A) and immune cells (B). ICs, immune cells; OS, overall survival; TCs, tumor cells.

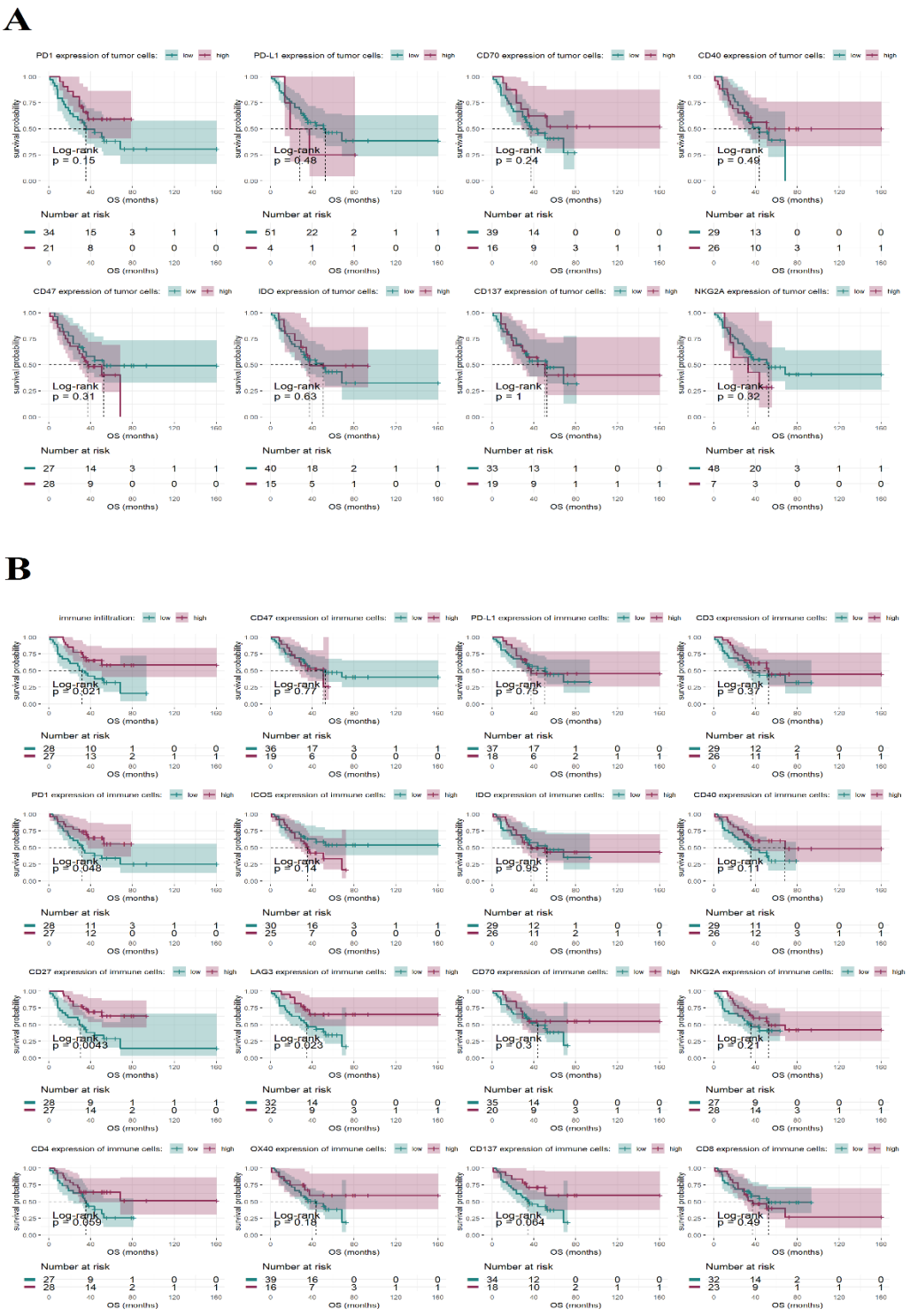

Figure 11. Effect of the expression pattern of immune-related markers on overall survival for LCNEC and SCLC. Kaplan-Meier estimates for OS concerning the expression pattern of immune-related markers by TCs (A) and immune cells (B). OS, overall survival.

4.2.3 Multivariate Cox-regression model for OS

A multivariate Cox regression analysis demonstrated that only age (p = 0.008) and vascular involvement (p = 0.012) independently affected OS across all three histological subtypes. Accordingly, older patients and those with vascular involvement experienced poorer survival outcomes (Figure 12A). Interestingly, when the analysis was restricted to LCNEC and SCLC patients, age remained an independent prognostic factor (p = 0.05), while the prognostic significance of vascular involvement was borderline (p = 0.06) (Figure 12B). Notably, none of the immune-related markers that were significant in the univariate models retained their significance in the multivariate analysis (Figure 12A and B).

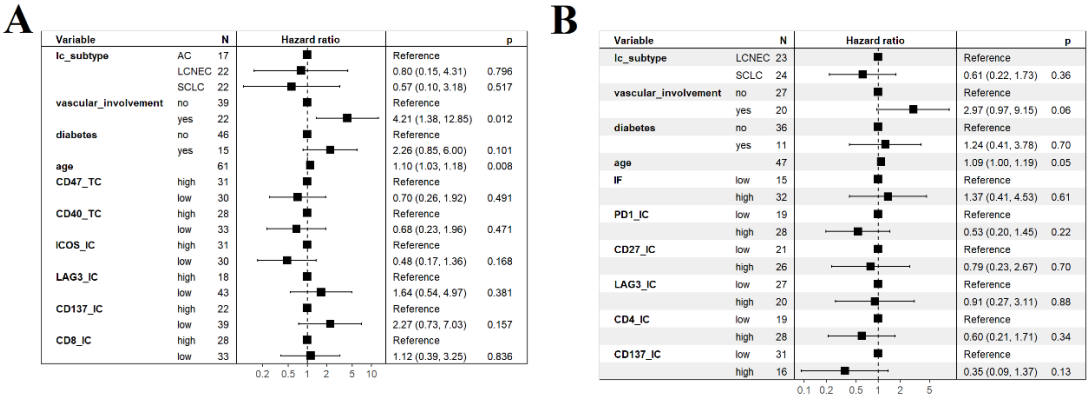

Figure 12. Multivariate Cox-regression model for OS including AC, LCNEC, and SCLC (A) or only LCNEC and SCLC (B). The outcomes are presented as hazard ratios (HR) and their corresponding 95% confidence intervals (CI). N indicates the number of samples in each category. P-values show the significance of the associations. lc_subtype, lung cancer_subtype; TC, tumor cell; IC, immune cell; AC, atypical carcinoid; LCNEC, large cell neuroendocrine carcinoma; SCLC, small cell lung cancer; IF, immune infiltration

DOI:10.14753/SE.2025.3289

4.2.4 Correlation between the expression patterns of immune-related markers defined by TCs and ICs

Figure 13 illustrates the statistically significant correlations between the evaluated markers and the overall abundance of immune infiltrates. Notably, tumor cell PD-1 expression correlated with CD70 expression in both immune and TCs ($R = 0.446$, $p^* = 0.0058$; $Rfilt = 0.6849$, $pfilt^* < 0.0001$). Similarly, a significant correlation was observed between the overall abundance of immune infiltrates and CD3 expression in ICs ($Rfilt = 0.6044$, $pfilt^* = 0.0206$). For PD-L1, a strong positive linear correlation was identified between tumor cell PD-L1 expression and LAG3 expression in ICs ($Rfilt = 0.8294$, $pfilt^* = 0.0008$).

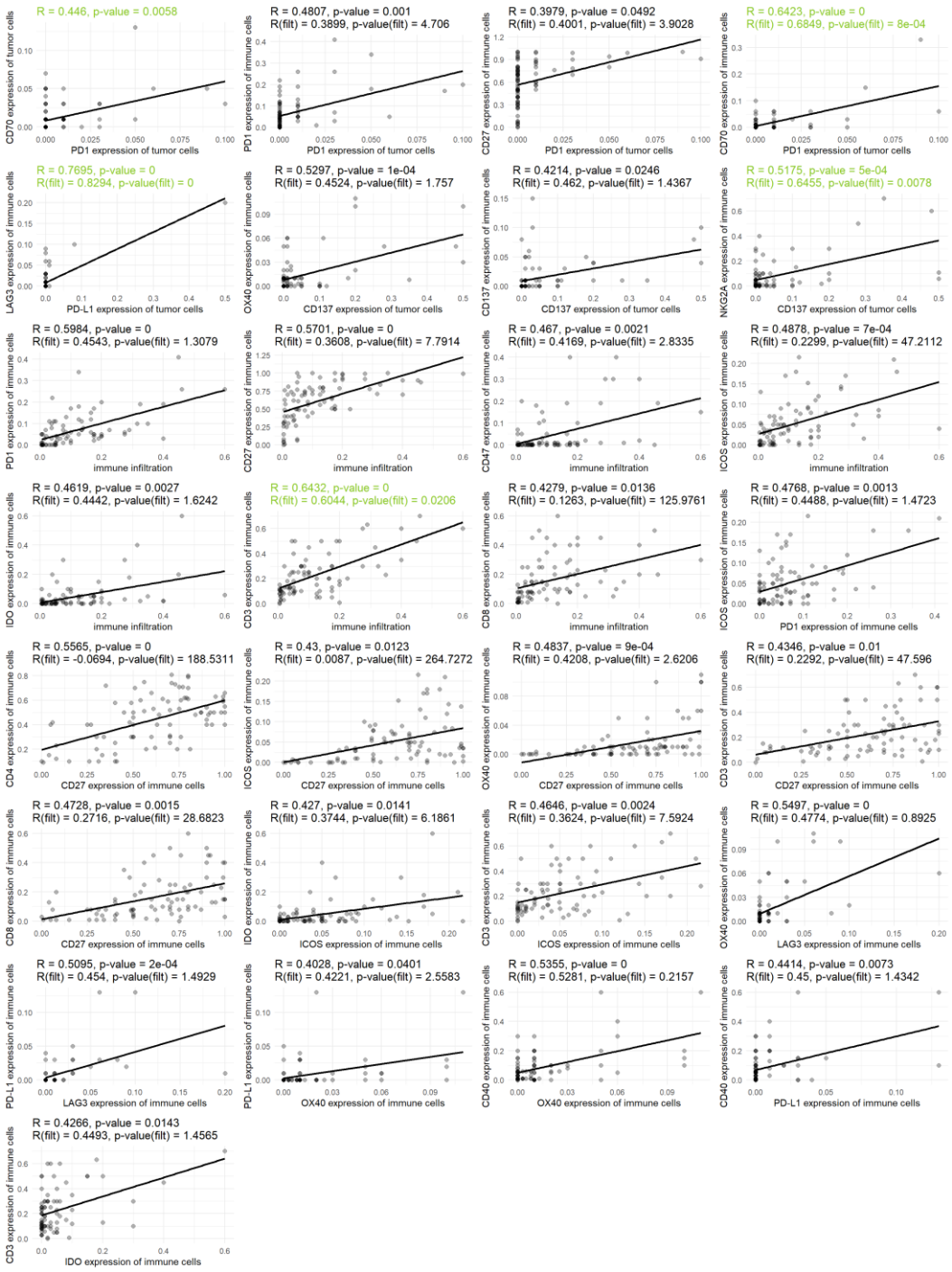

Figure 13. Correlation between expressions of immune-related markers in TCs and immune cells. Only associations significant after the Bonferroni correction are shown. All p-values are adjusted for multiple comparisons. Results obtained for a filtered dataset, including samples with an immune infiltration of 0.1 or larger, are indicated with "(filt)". The results are highlighted in green if the observed correlation remained significant on the filtered dataset. ICs, immune cells; TCs, tumor cells.

5. Discussion

As humans shape their environment, the environment affects humans. (93) With tumors, we have a similar case. (94) The ideal microenvironment is essential for SCLC's survival, adaptation, and growth, and exploring its characteristics and dynamics is crucial. (95)

SCLC tumors mostly spread to LNs as a first step of invasiveness due to their early metastatic capability. (96)

Precise diagnosis is mandatory for treating these malignancies, which can be acquired from different disease sites and with various approaches. (97) Recent studies showed that the molecular features of PTs often differ from matched LN metastases molecular landscape. Expression patterns of therapeutic targets and subtype markers can vary depending on their site of origin. (98) Expressions data from the RNAseq revealed no significant differences in PTs and their corresponding LN metastases. However, IHC staining revealed diverging results between these two origins. DLL3 and NEUROD1 showed different expression patterns in PTs compared to their paired LN metastases. A study in NSCLC has shown approximately 80% consistency between IHC and RNAseq findings. (99) After multiple testing corrections, the overall genomic landscape between PTs and LN metastases revealed five genes with considerable expression differences: PGC, FIGF, ROS1, CFTR and TMPRSS2. In LN metastases, these genes presented significant downregulation. *PGC* produces peroxisome proliferator-activated receptor gamma coactivator 1-alpha (PGC-1α), a key regulator of cellular energy metabolism; *FIGF* gene specifies vascular endothelial growth factors (VEGFs), which enhance angiogenesis and lymphangiogenesis; *ROS1* gene encodes a receptor tyrosine kinase involved in cell growth and differentiation. In cancer development, alterations and modulation of these receptors are significant steps for growth and survival. (100-103) NSCLC and various cancer are connected with *ROS1* mutation. (104, 105) The *TMPRSS2* gene produces a type II transmembrane protease widely expressed in epithelial cells in the respiratory tract. It acts as an intracellular transport for respiratory viral infections. Blocking this pathway is a widely investigated method. (106) Focusing on lung adenocarcinoma with reduced *TMPRSS2* expression impaired clinical outcomes revealed high oncogenic activity and boosted tumor growth. (107) The Cystic Fibrosis Transmembrane Conductance Regulator (*CFTR*) gene forms a cAMP-regulated channel,

the mutation of which leads to cystic fibrosis. However, it is less known that the *CFTR* functions as a tumor suppressor, and impaired *CFTR* promotes cancer progression. (108) Our study's IHC analysis demonstrated that the DLL3 expression was significantly higher in PTs than in the corresponding LN metastases. On the other hand, NEUROD1 expression was considerably lower in PTs than in matched LN metastases**.** The suppressed expression of DLL3 in LN metastases may result from various stages of gene regulation. (109) DLL3 is an inhibitory ligand of the Notch signaling pathway, which is highly expressed on the cell surface in SCLC and other high-grade NETs. (110, 111) This ligand is missing in healthy lung tissue and is found on the surface of SCLC tumors, which makes it a good candidate for a therapeutic target. It is currently under investigation in several clinical trials for SCLC. (112-114) A bispecific T-cell engager called tarlatamab is the most effective agent that is used in patients with previously treated SCLC. In a specific study, the overall response rate (ORR) of tarlatamab-treated patients was 40% (10 mg group) vs. 32% (100 mg group), with a median PFS of 4.9 vs. 3.9 months among 220 participants. The 9-month OS rates were 68% (10 mg) vs. 66% (100 mg). (115) These results led to a fast FDA approval for treating patients with previously treated, recurrent SCLC. (116) Not all trials have a clear path to validation. The TRINITY trial, assessed the effectiveness and safety of rovalpituzumab tesirine (Rova-T) in patients with relapsed or refractory SCLC. This agent is an antibody-drug conjugate targeting DLL3. ORR was 12.4%, with a median OS of 5.6 months in 339 participants. High DLL3 expression showed slightly better outcomes, with an ORR of 14.3% and an OS of 5.7 months. Rova-T had limited clinical benefit, and its use is linked to substantial grade 3–5 adverse events, which were seen in 63% of patients. (117) The newest approach targeting DLL3 originates from the field of hematological cancers, known as the chimeric antigen receptor T-cell (CAR-T) therapy. AMG 119 is one of the new CAR-T cell therapy targeting DLL3, developed for relapsed and refractory SCLC. Its first clinical pharmacology profiling trial showed substantial cellular expansion, prolonged persistence, and a favorable exposure-response relationship. It was well tolerated, with no dose-limiting toxicities observed. (118)

Although DLL3-targeting therapies are currently given to metastatic SCLC patients regardless of their DLL3 expression levels, evaluating patient-specific DLL3 expression could change clinical practices in the future. Profiling DLL3 expression in the PT should

be the priority because LN metastases may not fully mimic the expression profile of the lung lesion, as we have seen in our results. A novel DLL3-targeted imaging tracer ([89Zr]Zr-DFO-SC16.56) is being evaluated in the PET-CT setting. The 80% of evaluated NE cancers, including SCLC were DLL3-positive. The tracer uptake aligned with the DLL3 expression on IHC in 94% of cases. This new method requires further validation. However, the early non-invasive detection of DLL3 could potentially help the selection of suitable patients. (119)

Around 1985, the available studies could only separate SCLCs into two main subtypes based on their morphological characteristics: classic vs. variant. (129) Nevertheless, with the help of advanced molecular biology, four distinct transcriptional subtypes were identified in the late 2010s (SCLC-A, SCLC-N, SCLC-P, and SCLC-Y). Further research revealed that the expressions of the tumor mass have different subtype patterns, which are complex and multidimensional. (80, 81, 120) Our hierarchical clustering revealed five separate subtypes in PT and LN metastatic lesions (SCLC-A, -AN, -N, -P, and -QN). As other multiple independent analyses also found, no clear YAP1 subtype was observed in our cohort. (11, 80, 121-123) The lack of an SCLC-Y subtype might be attributed to tumor heterogeneity, therapy-induced plasticity, and technical controversies regarding the original classification. (80, 124-126) In the analysis of our cohort, significant changes were observed in subtype distribution between LN metastases and their matched PT. The detailed transitions we detected were SCLC-A to SCLC-AN or SCLC-N, while losing NE characteristics, and SCLC-P and SCLC-QN to SCLC-AN, SCLC-N, or SCLC-A, while acquiring dominant NE characteristics. SCLC-A usually acts as a precursor of the SCLC-N subtype, which observation can underscore these results. (82, 127) Another key aspect is the activation of Notch signal, which leads to the loss of NE differentiation. (128, 129) Aligning with other research findings, we have also identified a distinct SCLC-AN subtype, which could serve as support for this hypothesis. While none of our selected patients received neoadjuvant ChT, the dominant subtype expression is also likely shaped by systemic treatment responses and various mechanisms involved in metastatic progression. (76, 81, 86) In distinct metastasis a non-NE tumor can obtains NE characteristics, which transformation could originate from an existing NE component in the metastasis. Since NE TCs are more aggressive compared to those with low or absent NE features, they may be the primary drivers of forming LN metastasis. (11, 81)

Exploring deeper, SMARCA4 is a major regulator of SCLC, controlling the change between NE and non-NE phenotypes. SMARCA4 locks the NE state while modulating REST splicing through SRRM4, suppressing NE features and promoting the expression of ASCL1 and NEUROD1. SMARCA4's role in maintaining SCLC subtype plasticity is critical and could explain the results of our research. (130)

We must consider another important aspect when analyzing the tumor's microenvironment, which is the immune-related factor. (131) In our cohort high CD47 expression of TCs showed worse survival, whereas CD40 expression of TCs correlated with better outcomes. Investigating ICs expression, high CD137 was correlated with improved survival, whereas ICOS expression was associated with worse outcomes.

These findings are coherent with current literature regarding their role in tumor biology. CD47 is an important immune checkpoint that sends an antiphagocytic signal to macrophages while inhibiting neutrophil cytotoxicity. (132) In cancerous diseases that target the ovarium, endometrium, breast, pancreas, plus sarcomas and NSCLC, overexpresion of this checkpoint marker is commonly observed. According to other findings, elevated levels of CD47 correlated with an impaired prognosis. (133-138) These results gave a strong foundation for the development of a CD47-blocking peptide called VK30. When the peptid attaches to the CD47 receptor, it leads to increased apoptosis and improved macrophage phagocytosis. (139) The CD40/CD40L axis has a broad role in immunobiology. It modulates antigen-specific T and B cell activation, controls both immune pathways, and boosts NK cell activation. It is usually expressed in NSCLC, ovarian cancer, and pancreatic adenocarcinoma. (140) A study has shown better OS in melanoma patients with high CD40 expression. (141)

CD137 activates T cells and NK cells. Blocking their receptor was a potential goal; however, clinical testing raised concerns about toxicity. (142) ICOS is a receptor controlling immune regulation and tumor progression. ICOS is Janus-faced; some studies showed that in multiple cancers, ICOS expression influences immune cell infiltration and prognosis, particularly in lung adenocarcinoma. In these cases, higher ICOS levels correlate with a beneficial tumor immune microenvironment and improved survival. On the other hand, in lower-grade glioma and uveal melanoma, high ICOS expression resulted in an unfavorable prognosis (143)

Our study uncovered that only age and vascular involvement were independently associated with OS in AC, LCNEC, and SCLC. When these two factors are combined, survival outcomes get worse. Focusing only on LCNEC and SCLC, the patient's age remained as an independent prognostic factor. The complex role of immune markers in LNEN prognosis is well known, although their impact on survival remains unclear.

Some limitations in our study must be addressed. While the study material is notable due to the rarity of surgically resected tumor specimens in SCLC, the sample size remains moderate for expression analysis, and further validation studies are needed. Additionally, although RNA expression analysis was conducted on tissue samples carefully selected from the most viable tumor regions through macrodissection, non-malignant stromal components could still have a minor influence on RNAseq results. This limitation applies only to RNAseq data, as IHC staining was performed exclusively on TCs. Lastly, IHC expression levels in TMA samples could be affected by intratumoral heterogeneity. However, this was partially mitigated by including two distinct tissue cores from the same tumor in each TMA used in our study.

When analyzing the immunophenotypic differences in LNENs, the overall study cohort remained small despite successfully collecting many surgically treated samples suitable for profiling studies. The study's retrospective nature also presents limitations, as the collection of clinicopathological data, follow-up information, and cancer-specific survival data was not complete in certain cases. The effects of immunotherapy are not being investigated in our study, as it includes only surgically treated patients. While we analyzed whole tissue sections from surgical specimens and examined ten randomly selected areas per sample, the potential impact of tumor heterogeneity must be considered when interpreting our results.

DOI:10.14753/SE.2025.3289

6. Conclusions

Both studies aim to provide a deeper understanding of tumor heterogeneity in LNENs. Firstly, we gained insights into the molecular changes during metastatic spread by analyzing a cohort of surgically resected primary SCLCs and their LN metastases. Different expressions of DLL3 and NEUROD1 were seen in the PTs and paired LN metastases. DLL3 was significantly higher in PTs, whereas NEUROD1 was more strongly expressed in LN metastases. Our results imply that the molecular subtype of LN metastases does not always align with the same PT, pointing to potential subtype transitions during lymphatic dissemination. Changes from both NE subtypes to non-NE lesions and non-NE subtypes to NE subtypes were seen. Through these lenses, potential diagnostic challenges emerge when determining the molecular profile and classification of SCLCs based solely on LN biopsies.

Secondly, we obtained a large panel of immune-related markers and investigated the immunologic profiles and expression patterns of LNENs. TCs elevated CD47 expression showed impaired survival, while high CD40 expression correlated with improved outcomes. As we investigated immune cells, high expression of CD137 improved patient survival, whereas high expression of ICOS was associated with worse patient outcomes. Our analyses revealed that higher age and vascular involvement were independently associated with impaired OS in AC, LCNEC, and SCLC. Age remained an independent prognostic factor when the analysis focused only on LCNEC and SCLC patients.

DOI:10.14753/SE.2025.3289

7. Summary

Targeted therapy made a big leap in the treatment of cancerous diseases, but this option needs more precise and advanced diagnosis. Despite being the deadliest subtype of lung cancer, SCLC treatment lags behind that of other lung cancer types. Development of new therapeutic agents needs a detailed landscape of SCLC molecular subtypes, both concerning PTs and LN metastases. Our study profiled 32 surgically resected SCLCs and corresponding LN metastases with RNASeq and IHC. The RNA expression profile showed no differences between primary tumors and their paired LN metastases; however, key differences emerged when the samples were examined by IHC. Specifically, DLL3 expression was significantly higher in the primary tumors than in corresponding LN metastases, whereas NEUROD1 expression was significantly lower in the LN metastatic lesions. A change in molecular subtype in the context of primary tumors – LN metastases was seen in 21 cases. We continued with a broader investigation, analyzing the immunologic profiles and expression patterns of LNENs. We identified several immunomarkers that influenced survival. Elevated CD40 and CD137 expression was associated with improved patient survival, while high CD47 and ICOS expression correlated with worse patient outcomes. When we focused solely on the data of LCNEC and SCLC, older age and vascular involvement was associated with significantly worse survival. Further examination confirmed age as a key prognostic factor. According to these findings, investigating LNENs requires a comprehensive clinical approach since tumors from different sites show distinct phenotypes and immunologic landscapes that can influence patient outcomes.

8. References

1. Bray F, Laversanne M, Sung H, Ferlay J, Siegel RL, Soerjomataram I, et al. Global cancer statistics 2022: GLOBOCAN estimates of incidence and mortality worldwide for 36 cancers in 185 countries. CA Cancer J Clin. 2024;74(3):229-63.

2. Galffy G, Szabo GT, Tamasi L, Muller V, Moldvay J, Sarosi V, et al. Decreasing incidence and mortality of lung cancer in Hungary between 2011 and 2021 revealed by robust estimates reconciling multiple data sources. Pathol Oncol Res. 2024;30:1611754.

3. Guida F, Kidman R, Ferlay J, Schuz J, Soerjomataram I, Kithaka B, et al. Global and regional estimates of orphans attributed to maternal cancer mortality in 2020. Nat Med. 2022;28(12):2563-72.

4. Bergman AS, Axberg U, Hanson E. When a parent dies - a systematic review of the effects of support programs for parentally bereaved children and their caregivers. BMC Palliat Care. 2017;16(1):39.

5. Li J, Vestergaard M, Cnattingius S, Gissler M, Bech BH, Obel C, et al. Mortality after parental death in childhood: a nationwide cohort study from three Nordic countries. PLoS Med. 2014;11(7):e1001679.

6. Rostila M, Saarela JM. Time Does Not Heal All Wounds: Mortality Following the Death of a Parent. Journal of Marriage and Family. 2011;73(1):236-49.

7. Curado M, Edwards B, Shin H, Storm H, Ferlay J, Heanue M, et al. Cancer incidence in five continents, vol. IX: IARC scientific publications Lyon; 2007.

8. Zappa C, Mousa SA. Non-small cell lung cancer: current treatment and future advances. Transl Lung Cancer Res. 2016;5(3):288-300.

9. George J, Lim JS, Jang SJ, Cun Y, Ozretic L, Kong G, et al. Comprehensive genomic profiles of small cell lung cancer. Nature. 2015;524(7563):47-53.

10. Rekhtman N. Neuroendocrine tumors of the lung: an update. Arch Pathol Lab Med. 2010;134(11):1628-38.

11. Megyesfalvi Z, Gay CM, Popper H, Pirker R, Ostoros G, Heeke S, et al. Clinical insights into small cell lung cancer: Tumor heterogeneity, diagnosis, therapy, and future directions. CA Cancer J Clin. 2023;73(6):620-52.

12. Nicholson AG, Tsao MS, Beasley MB, Borczuk AC, Brambilla E, Cooper WA, et al. The 2021 WHO Classification of Lung Tumors: Impact of Advances Since 2015. J Thorac Oncol. 2022;17(3):362-87.

13. Board WCoTE. Thoracic tumours. 5th ed. Lyon (France): International Agency for Research on Cancer; 2021.

14. Fisseler-Eckhoff A, Demes M. Neuroendocrine tumors of the lung. Cancers (Basel). 2012;4(3):777-98.

15. Shah S, Gosain R, Groman A, Gosain R, Dasari A, Halfdanarson TR, et al. Incidence and Survival Outcomes in Patients with Lung Neuroendocrine Neoplasms in the United States. Cancers (Basel). 2021;13(8):1753.

16. Dasari A, Shen C, Halperin D, Zhao B, Zhou S, Xu Y, et al. Trends in the Incidence, Prevalence, and Survival Outcomes in Patients With Neuroendocrine Tumors in the United States. JAMA Oncol. 2017;3(10):1335-42.

17. Hallet J, Law CH, Cukier M, Saskin R, Liu N, Singh S. Exploring the rising incidence of neuroendocrine tumors: a population-based analysis of epidemiology, metastatic presentation, and outcomes. Cancer. 2015;121(4):589-97.

18. Broder MS, Cai B, Chang E, Neary MP. Incidence and prevalence of neuroendocrine tumors of the lung: analysis of a US commercial insurance claims database. BMC Pulm Med. 2018;18(1):135.

19. Dam G, Gronbaek H, Sundlov A, Botling J, Sundin A, Petersen RH, et al. Nordic 2023 guidelines for the diagnosis and treatment of lung neuroendocrine neoplasms. Acta Oncol. 2023;62(5):431-7.

20. Kalemkerian GP, Schneider BJ. Advances in Small Cell Lung Cancer. Hematol Oncol Clin North Am. 2017;31(1):143-56.

21. Thomas R, Christopher DJ, Balamugesh T, Shah A. Clinico-pathologic study of pulmonary carcinoid tumours--a retrospective analysis and review of literature. Respir Med. 2008;102(11):1611-4.

22. Granberg D, Juhlin CC, Falhammar H, Hedayati E. Lung Carcinoids: A Comprehensive Review for Clinicians. Cancers (Basel). 2023;15(22).

23. George J, Lim JS, Jang SJ. Comprehensive genomic profiles of small cell lung cancer. Nature. 2015;524:47-53.

24. Schwendenwein A, Megyesfalvi Z, Barany N. Molecular profiles of small cell lung cancer subtypes: therapeutic implications. Molecular therapy oncolytics. 2021;20.

25. Khuder SA. Effect of cigarette smoking on major histological types of lung cancer: a meta-analysis. Lung Cancer. 2001;31(2-3):139-48.

26. Pleasance ED, Stephens PJ, O'Meara S, McBride DJ, Meynert A, Jones D, et al. A small-cell lung cancer genome with complex signatures of tobacco exposure. Nature. 2010;463(7278):184-90.

27. Travis WD, Brambilla E, Müller-Hermelink HK, Harris CC. Pathology and Genetics of Tumours of the Lung, Pleura, Thymus and Heart. Lyon, France: IARC Press; 2004.

28. Travis WD, Brambilla E, Burke AP, Marx A, Nicholson AG. WHO Classification of Tumours of the Lung, Pleura, Thymus and Heart. Lyon, France: International Agency for Research on Cancer (IARC); 2015.

29. Cree IA, Tan PH, Travis WD, Wesseling P, Yagi Y, White VA, et al. Counting mitoses: SI(ze) matters! Mod Pathol. 2021;34(9):1651-7.

30. Iams WT, Shiuan E, Meador CB, Roth M, Bordeaux J, Vaupel C, et al. Improved Prognosis and Increased Tumor-Infiltrating Lymphocytes in Patients Who Have SCLC With Neurologic Paraneoplastic Syndromes. J Thorac Oncol. 2019;14(11):1970-81.

31. Soomro Z, Youssef M, Yust-Katz S, Jalali A, Patel AJ, Mandel J. Paraneoplastic syndromes in small cell lung cancer. J Thorac Dis. 2020;12(10):6253-63.

32. Gade AK, Olariu E, Douthit NT. Carcinoid Syndrome: A Review. Cureus. 2020;12(3):e7186.

33. Savu C, Melinte A, Diaconu C, Stiru O, Gherghiceanu F, Tudorica Ș DO, et al. Lung neuroendocrine tumors: A systematic literature review (Review). Exp Ther Med. 2022;23(2):176.

34. Travis WD. Lung Cancer Pathology: Current Concepts. Clin Chest Med. 2020;41(1):67-85.

35. Fasano M, Della Corte CM, Papaccio F, Ciardiello F, Morgillo F. Pulmonary Large-Cell Neuroendocrine Carcinoma: From Epidemiology to Therapy. J Thorac Oncol. 2015;10(8):1133-41.

36. Kanaji N, Watanabe N, Kita N, Bandoh S, Tadokoro A, Ishii T, et al. Paraneoplastic syndromes associated with lung cancer. World J Clin Oncol. 2014;5(3):197-223.

37. National Comprehensive Cancer N. NCCN Guidelines Version 2.2025: Small Cell Lung Cancer. Fort Washington, PA: National Comprehensive Cancer Network; 2025.

38. Roesel C, Welter S, Kambartel KO, Weinreich G, Krbek T, Serke M, et al. Prognostic markers in resected large cell neuroendocrine carcinoma: a multicentre retrospective analysis. J Thorac Dis. 2020;12(3):466-76.

39. Megyesfalvi Z, Gay CM, Popper H, Pirker R, Ostoros G, Heeke S, et al. Clinical insights into small cell lung cancer: Tumor heterogeneity, diagnosis, therapy, and future directions. CA: A Cancer Journal for Clinicians.n/a(n/a).

40. Boushey RP, Dackiw AP. Carcinoid tumors. Curr Treat Options Oncol. 2002;3(4):319-26.

41. Caplin ME, Pavel M, Ćwikła JB, Phan AT, Raderer M, Sedláčková E, et al. Lanreotide in metastatic enteropancreatic neuroendocrine tumors. New England Journal of Medicine. 2014;371(3):224-33.

42. Rinke A, Müller H-H, Schade-Brittinger C, Klose K-J, Barth P, Wied M, et al. Placebo-controlled, double-blind, prospective, randomized study on the effect of octreotide LAR in the control of tumor growth in patients with metastatic neuroendocrine midgut tumors: a report from the PROMID Study Group. Journal of Clinical oncology. 2009;27(28):4656-63.

43. Dingemans AC, Fruh M, Ardizzoni A, Besse B, Faivre-Finn C, Hendriks LE, et al. Small-cell lung cancer: ESMO Clinical Practice Guidelines for diagnosis, treatment and follow-up(☆). Ann Oncol. 2021;32(7):839-53.

44. Oberg K, Hellman P, Ferolla P, Papotti M, Group EGW. Neuroendocrine bronchial and thymic tumors: ESMO Clinical Practice Guidelines for diagnosis, treatment and follow-up. Ann Oncol. 2012;23 Suppl 7:vii120-3.

45. Soldath P, Petersen RH. The Surgical Management of Lung Neuroendocrine Neoplasms. Cancers (Basel). 2023;15(6).

46. National Comprehensive Cancer N. NCCN Clinical Practice Guidelines in Oncology: Neuroendocrine Tumors (Version 2.2024).

47. Lababede O, Meziane MA. The Eighth Edition of TNM Staging of Lung Cancer: Reference Chart and Diagrams. Oncologist. 2018;23(7):844-8.

48. Detterbeck FC. The eighth edition TNM stage classification for lung cancer: What does it mean on main street? J Thorac Cardiovasc Surg. 2018;155(1):356-9.

49. Detterbeck FC, Woodard GA, Bader AS, Dacic S, Grant MJ, Park HS, et al. The Proposed Ninth Edition TNM Classification of Lung Cancer. Chest. 2024;166(4):882-95.

50. Micke P, Faldum A, Metz T, Beeh KM, Bittinger F, Hengstler JG, et al. Staging small cell lung cancer: Veterans Administration Lung Study Group versus International Association for the Study of Lung Cancer--what limits limited disease? Lung Cancer. 2002;37(3):271-6.

51. Anraku M, Waddell TK. Surgery for small-cell lung cancer. Semin Thorac Cardiovasc Surg. 2006;18(3):211-6.

52. Hoda MA, Klikovits T, Klepetko W. Controversies in oncology: surgery for small cell lung cancer? It's time to rethink the case. ESMO Open. 2018;3(3):e000366.

53. Gazdar A, Bunn P, Minna J. Small-cell lung cancer: what we know, what we need to know and the path forward. Nature reviews Cancer. 2017;17.

54. Chan JM, Quintanal-Villalonga A, Gao VR, Xie Y, Allaj V, Chaudhary O, et al. Signatures of plasticity, metastasis, and immunosuppression in an atlas of human small cell lung cancer. Cancer Cell. 2021;39(11):1479-96 e18.

55. National Comprehensive Cancer N. NCCN Clinical Practice Guidelines in Oncology: Small Cell Lung Cancer (Version 2.2024). 2024.

56. Counago F, de la Pinta C, Gonzalo S, Fernandez C, Almendros P, Calvo P, et al. GOECP/SEOR radiotherapy guidelines for small-cell lung cancer. World J Clin Oncol. 2021;12(3):115-43.

57. Di Molfetta S, Feola T, Fanciulli G, Florio T, Colao A, Faggiano A, et al. Immune Checkpoint Blockade in Lung Carcinoids with Aggressive Behaviour: One More Arrow in Our Quiver? J Clin Med. 2022;11(4).

58. Lokich JJ. The frequency and clinical biology of the ectopic hormone syndromes of small cell carcinoma. Cancer. 1982;50(10):2111-4.

59. Iyer P, Ibrahim M, Siddiqui W, Dirweesh A. Syndrome of inappropriate secretion of anti-diuretic hormone (SIADH) as an initial presenting sign of non small cell lung cancer-case report and literature review. Respir Med Case Rep. 2017;22:164-7.

60. Ferolla P, Brizzi MP, Meyer T, Mansoor W, Mazieres J, Do Cao C, et al. Efficacy and safety of long-acting pasireotide or everolimus alone or in combination in patients with advanced carcinoids of the lung and thymus (LUNA): an open-label, multicentre, randomised, phase 2 trial. Lancet Oncol. 2017;18(12):1652-64.

61. Berghmans T, Dingemans AM, Hendriks LEL, Cadranel J. Immunotherapy for nonsmall cell lung cancer: a new therapeutic algorithm. Eur Respir J. 2020;55(2).

62. Bremnes RM, Busund LT, Kilvær TL, Andersen S, Richardsen E, Paulsen EE, et al. The Role of Tumor-Infiltrating Lymphocytes in Development, Progression, and Prognosis of Non-Small Cell Lung Cancer. J Thorac Oncol. 2016;11(6):789-800.

63. Dantoing E, Piton N, Salaün M, Thiberville L, Guisier F. Anti-PD1/PD-L1 Immunotherapy for Non-Small Cell Lung Cancer with Actionable Oncogenic Driver Mutations. Int J Mol Sci. 2021;22(12).

64. Han Y, Liu D, Li L. PD-1/PD-L1 pathway: current researches in cancer. Am J Cancer Res. 2020;10(3):727-42.

65. Pavan A, Attili I, Pasello G, Guarneri V, Conte PF, Bonanno L. Immunotherapy in small-cell lung cancer: from molecular promises to clinical challenges. J Immunother Cancer. 2019;7(1):205.

66. Rowshanravan B, Halliday N, Sansom DM. CTLA-4: a moving target in immunotherapy. Blood. 2018;131(1):58-67.

67. Horn L, Mansfield AS, Szczęsna A, Havel L, Krzakowski M, Hochmair MJ, et al. First-Line Atezolizumab plus Chemotherapy in Extensive-Stage Small-Cell Lung Cancer. New England Journal of Medicine. 2018;379(23):2220-9.

68. Paz-Ares L, Dvorkin M, Chen Y, Reinmuth N, Hotta K, Trukhin D, et al. Durvalumab plus platinum-etoposide versus platinum-etoposide in first-line treatment of extensive-stage small-cell lung cancer (CASPIAN): a randomised, controlled, open-label, phase 3 trial. Lancet. 2019;394(10212):1929-39.

69. Xiong W, Zhao Y, Du H, Guo X. Current Status of Immune Checkpoint Inhibitor Immunotherapy for Lung Cancer. Frontiers in Oncology. 2021;11.

70. Onoi K, Chihara Y, Uchino J, Shimamoto T, Morimoto Y, Iwasaku M, et al. Immune Checkpoint Inhibitors for Lung Cancer Treatment: A Review. Journal of Clinical Medicine. 2020;9(5):1362.

71. Chan S, Belmar N, Ho S, Rogers B, Stickler M, Graham M, et al. An anti-PD-1-GITR-L bispecific agonist induces GITR clustering-mediated T cell activation for cancer immunotherapy. Nat Cancer. 2022;3(3):337-54.

72. Hernandez-Guerrero T, Moreno V. GITR Antibodies in Cancer: Not Ready for Prime Time. Clin Cancer Res. 2022;28(18):3905-7.

73. Gazdar AF, Carney DN, Nau MM, Minna JD. Characterization of variant subclasses of cell lines derived from small cell lung cancer having distinctive biochemical, morphological, and growth properties. Cancer Res. 1985;45(6):2924-30.

74. Kandel S, Adhikary P, Li G, Cheng K. The TIM3/Gal9 signaling pathway: An emerging target for cancer immunotherapy. Cancer Lett. 2021;510:67-78.

75. Solinas C, De Silva P, Bron D, Willard-Gallo K, Sangiolo D. Significance of TIM3 expression in cancer: From biology to the clinic. Semin Oncol. 2019;46(4-5):372-9.

76. Gay CM, Stewart CA, Park EM, Diao L, Groves SM, Heeke S, et al. Patterns of transcription factor programs and immune pathway activation define four major subtypes of SCLC with distinct therapeutic vulnerabilities. Cancer Cell. 2021;39(3):346-60.e7.

77. Rudin C, Poirier J, Byers L. Molecular subtypes of small cell lung cancer: a synthesis of human and mouse model data. Nature reviews Cancer. 2019;19.

78. Megyesfalvi Z, Barany N, Valko Z, Bugyik E, Paku S, Berta J, et al. [Heterogeneity of small cell lung cancer: biological and clinicopathological implications]. Magy Onkol. 2020;64(3):243-55.

79. Rudin CM, Poirier JT, Byers LA, Dive C, Dowlati A, George J, et al. Molecular subtypes of small cell lung cancer: a synthesis of human and mouse model data. Nat Rev Cancer. 2019;19(5):289-97.

80. Baine MK, Hsieh MS, Lai WV, Egger JV, Jungbluth AA, Daneshbod Y, et al. SCLC Subtypes Defined by ASCL1, NEUROD1, POU2F3, and YAP1: A Comprehensive Immunohistochemical and Histopathologic Characterization. J Thorac Oncol. 2020;15(12):1823-35.

81. Megyesfalvi Z, Barany N, Lantos A, Valko Z, Pipek O, Lang C, et al. Expression patterns and prognostic relevance of subtype-specific transcription factors in surgically resected small-cell lung cancer: an international multicenter study. J Pathol. 2022;257(5):674-86.

82. Borromeo MD, Savage TK, Kollipara RK, He M, Augustyn A, Osborne JK, et al. ASCL1 and NEUROD1 Reveal Heterogeneity in Pulmonary Neuroendocrine Tumors and Regulate Distinct Genetic Programs. Cell Rep. 2016;16(5):1259-72.

83. Huang YH, Klingbeil O, He XY, Wu XS, Arun G, Lu B, et al. POU2F3 is a master regulator of a tuft cell-like variant of small cell lung cancer. Genes Dev. 2018;32(13-14):915-28.

84. Jimbo N, Ohbayashi C, Takeda M, Fujii T, Mitsui S, Tsukamoto R, et al. POU2F3-Expressing Small Cell Lung Carcinoma and Large Cell Neuroendocrine Carcinoma Show Morphologic and Phenotypic Overlap. Am J Surg Pathol. 2024;48(1):4-15.

85. Baine MK, Febres-Aldana CA, Chang JC, Jungbluth AA, Sethi S, Antonescu CR, et al. POU2F3 in SCLC: Clinicopathologic and Genomic Analysis With a Focus on Its Diagnostic Utility in Neuroendocrine-Low SCLC. J Thorac Oncol. 2022;17(9):1109-21.

86. Lohinai Z, Megyesfalvi Z, Suda K, Harko T, Ren S, Moldvay J, et al. Comparative expression analysis in small cell lung carcinoma reveals neuroendocrine pattern change in primary tumor versus lymph node metastases. Transl Lung Cancer Res. 2019;8(6):938-50.

87. Battifora H. The multitumor (sausage) tissue block: novel method for immunohistochemical antibody testing. Lab Invest. 1986;55(2):244-8.

88. Aspeslagh S, Postel-Vinay S, Rusakiewicz S, Soria JC, Zitvogel L, Marabelle A. Rationale for anti-OX40 cancer immunotherapy. Eur J Cancer. 2016;52:50-66.

89. Borst J, Ahrends T, Babala N, Melief CJM, Kastenmuller W. CD4(+) T cell help in cancer immunology and immunotherapy. Nat Rev Immunol. 2018;18(10):635-47.

90. Borst L, Sluijter M, Sturm G, Charoentong P, Santegoets SJ, van Gulijk M, et al. NKG2A is a late immune checkpoint on CD8 T cells and marks repeated stimulation and cell division. International Journal of Cancer. 2021;150(4):688-704.

91. Dora D, Rivard C, Yu H, Bunn P, Suda K, Ren S, et al. Neuroendocrine subtypes of small cell lung cancer differ in terms of immune microenvironment and checkpoint molecule distribution. Mol Oncol. 2020;14(9):1947-65.

92. Etxeberria I, Glez-Vaz J, Teijeira A, Melero I. New emerging targets in cancer immunotherapy: CD137/4-1BB costimulatory axis. ESMO Open. 2020;4(Suppl 3):e000733.

93. Rising J, Tedesco M, Piontek F, Stainforth DA. The missing risks of climate change. Nature. 2022;610(7933):643-51.

94. Binnewies M, Roberts EW, Kersten K, Chan V, Fearon DF, Merad M, et al. Understanding the tumor immune microenvironment (TIME) for effective therapy. Nat Med. 2018;24(5):541-50.

95. Desai P, Takahashi N, Kumar R, Nichols S, Malin J, Hunt A, et al. Microenvironment shapes small-cell lung cancer neuroendocrine states and presents therapeutic opportunities. Cell Rep Med. 2024;5(6):101610.

96. Zhang S, Chen J, Zhang R, Xu L, Wang Y, Yuan Z, et al. Pulmonary neuroendocrine tumors: study of 266 cases focusing on clinicopathological characteristics, immunophenotype, and prognosis. J Cancer Res Clin Oncol. 2023;149(3):1063-77.

97. Rivera MP, Mehta AC, Wahidi MM. Establishing the diagnosis of lung cancer: Diagnosis and management of lung cancer, 3rd ed: American College of Chest Physicians evidence-based clinical practice guidelines. Chest. 2013;143(5 Suppl):e142S-e65S.

98. Zhu Y, Ren W, Li S, Wu J, Hu X, Wang H, et al. Heterogeneity of molecular subtyping and therapy-related marker expression in primary tumors and paired lymph node metastases of small cell lung cancer. Virchows Arch. 2024.

99. Nesline MK, Previs RA, Dy GK, Deng L, Lee YH, DePietro P, et al. PD-L1 Expression by RNA-Sequencing in Non-Small Cell Lung Cancer: Concordance with Immunohistochemistry and Associations with Pembrolizumab Treatment Outcomes. Cancers (Basel). 2023;15(19):4789.

100. Bost F, Kaminski L. The metabolic modulator PGC-1alpha in cancer. Am J Cancer Res. 2019;9(2):198-211.

101. Liberti MV, Locasale JW. The Warburg Effect: How Does it Benefit Cancer Cells? Trends Biochem Sci. 2016;41(3):211-8.

102. Bailey E, Cui Y, Casey A, Stoler JM, Ai X, Ma D, et al. Pulmonary Vasculopathy Associated with FIGF Gene Mutation. Am J Pathol. 2017;187(1):25-32.

103. Bergethon K, Shaw AT, Ou SH, Katayama R, Lovly CM, McDonald NT, et al. ROS1 rearrangements define a unique molecular class of lung cancers. J Clin Oncol. 2012;30(8):863-70.

104. Takeuchi K, Soda M, Togashi Y, Suzuki R, Sakata S, Hatano S, et al. RET, ROS1 and ALK fusions in lung cancer. Nat Med. 2012;18(3):378-81.

105. Davies KD, Le AT, Theodoro MF, Skokan MC, Aisner DL, Berge EM, et al. Identifying and targeting ROS1 gene fusions in non-small cell lung cancer. Clin Cancer Res. 2012;18(17):4570-9.

106. Wettstein L, Kirchhoff F, Munch J. The Transmembrane Protease TMPRSS2 as a Therapeutic Target for COVID-19 Treatment. Int J Mol Sci. 2022;23(3).

107. Liu Z, Lu Q, Zhang Z, Feng Q, Wang X. TMPRSS2 is a tumor suppressor and its downregulation promotes antitumor immunity and immunotherapy response in lung adenocarcinoma. Respir Res. 2024;25(1):238.

108. Amaral MD, Quaresma MC, Pankonien I. What Role Does CFTR Play in Development, Differentiation, Regeneration and Cancer? Int J Mol Sci. 2020;21(9):3133.

109. Sorokin M, Ignatev K, Poddubskaya E, Vladimirova U, Gaifullin N, Lantsov D, et al. RNA Sequencing in Comparison to Immunohistochemistry for Measuring Cancer Biomarkers in Breast Cancer and Lung Cancer Specimens. Biomedicines. 2020;8(5):114.

110. Sabari JK, Lok BH, Laird JH, Poirier JT, Rudin CM. Unravelling the biology of SCLC: implications for therapy. Nat Rev Clin Oncol. 2017;14(9):549-61.

111. Saunders LR, Bankovich AJ, Anderson WC, Aujay MA, Bheddah S, Black K, et al. A DLL3-targeted antibody-drug conjugate eradicates high-grade pulmonary neuroendocrine tumor-initiating cells in vivo. Sci Transl Med. 2015;7(302):302ra136.

112. Huang J, Cao D, Sha J, Zhu X, Han S. DLL3 is regulated by LIN28B and miR-518d-5p and regulates cell proliferation, migration and chemotherapy response in advanced small cell lung cancer. Biochem Biophys Res Commun. 2019;514(3):853-60.

113. Serrano AG, Rocha P, Freitas Lima C, Stewart A, Zhang B, Diao L, et al. Delta-like ligand 3 (DLL3) landscape in pulmonary and extra-pulmonary neuroendocrine neoplasms. NPJ Precis Oncol. 2024;8(1):268.

114. Yao J, Bergsland E, Aggarwal R, Aparicio A, Beltran H, Crabtree JS, et al. DLL3 as an Emerging Target for the Treatment of Neuroendocrine Neoplasms. Oncologist. 2022;27(11):940-51.

115. Ahn MJ, Cho BC, Felip E, Korantzis I, Ohashi K, Majem M, et al. Tarlatamab for Patients with Previously Treated Small-Cell Lung Cancer. N Engl J Med. 2023;389(22):2063-75.

116. Administration USFD. FDA grants accelerated approval to tarlatamab-dlle for extensive stage small cell lung cancer https://www.fda.gov/drugs/resources-information-

approved-drugs/fda-grants-accelerated-approval-tarlatamab-dlle-extensive-stage-small-cell-lung-cancer2024 [

117. Morgensztern D, Besse B, Greillier L, Santana-Davila R, Ready N, Hann CL, et al. Efficacy and Safety of Rovalpituzumab Tesirine in Third-Line and Beyond Patients with DLL3-Expressing, Relapsed/Refractory Small-Cell Lung Cancer: Results From the Phase II TRINITY Study. Clin Cancer Res. 2019;25(23):6958-66.

118. Zhou D, Byers LA, Sable B, Smit MD, Sadraei NH, Dutta S, et al. Clinical Pharmacology Profile of AMG 119, the First Chimeric Antigen Receptor T (CAR-T) Cell Therapy Targeting Delta-Like Ligand 3 (DLL3), in Patients with Relapsed/Refractory Small Cell Lung Cancer (SCLC). J Clin Pharmacol. 2024;64(3):362-70.

119. Tendler S, Dunphy MP, Agee M, O'Donoghue J, Aly RG, Choudhury NJ, et al. Imaging with [(89)Zr]Zr-DFO-SC16.56 anti-DLL3 antibody in patients with high-grade neuroendocrine tumours of the lung and prostate: a phase 1/2, first-in-human trial. Lancet Oncol. 2024;25(8):1015-24.

120. Qi J, Zhang J, Liu N, Zhao L, Xu B. Prognostic Implications of Molecular Subtypes in Primary Small Cell Lung Cancer and Their Correlation With Cancer Immunity. Front Oncol. 2022;12:779276.

121. Park S, Hong TH, Hwang S, Heeke S, Gay CM, Kim J, et al. Comprehensive analysis of transcription factor-based molecular subtypes and their correlation to clinical outcomes in small-cell lung cancer. EBioMedicine. 2024;102:105062.

122. Chiang CL, Huang HC, Luo YH, Shen CI, Chao HS, Tseng YH, et al. Clinical utility of immunohistochemical subtyping in patients with small cell lung cancer. Lung Cancer. 2024;188:107473.

123. Caeser R, Egger JV, Chavan S, Socci ND, Jones CB, Kombak FE, et al. Genomic and transcriptomic analysis of a library of small cell lung cancer patient-derived xenografts. Nat Commun. 2022;13(1):2144.

124. Chen P, Sun C, Wang H, Zhao W, Wu Y, Guo H, et al. YAP1 expression is associated with survival and immunosuppression in small cell lung cancer. Cell Death Dis. 2023;14(9):636.

125. Redin E, Quintanal-Villalonga A, Rudin CM. Small cell lung cancer profiling: an updated synthesis of subtypes, vulnerabilities, and plasticity. Trends Cancer. 2024;10(10):935-46.

126. Ng J, Cai L, Girard L, Prall OWJ, Rajan N, Khoo C, et al. Molecular and Pathologic Characterization of YAP1-Expressing Small Cell Lung Cancer Cell Lines Leads to Reclassification as SMARCA4-Deficient Malignancies. Clin Cancer Res. 2024;30(9):1846-58.

127. Mollaoglu G, Guthrie MR, Bohm S, Bragelmann J, Can I, Ballieu PM, et al. MYC Drives Progression of Small Cell Lung Cancer to a Variant Neuroendocrine Subtype with Vulnerability to Aurora Kinase Inhibition. Cancer Cell. 2017;31(2):270-85.

128. Lim JS, Ibaseta A, Fischer MM, Cancilla B, O'Young G, Cristea S, et al. Intratumoural heterogeneity generated by Notch signalling promotes small-cell lung cancer. Nature. 2017;545(7654):360-4.

129. Meder L, Konig K, Ozretic L, Schultheis AM, Ueckeroth F, Ade CP, et al. NOTCH, ASCL1, p53 and RB alterations define an alternative pathway driving neuroendocrine and small cell lung carcinomas. Int J Cancer. 2016;138(4):927-38.

130. Redin E, Sridhar H, Zhan YA, Pereira Mello B, Zhong H, Durani V, et al. SMARCA4 controls state plasticity in small cell lung cancer through regulation of neuroendocrine transcription factors and REST splicing. J Hematol Oncol. 2024;17(1):58.

131. Wei R, Liu S, Zhang S, Min L, Zhu S. Cellular and Extracellular Components in Tumor Microenvironment and Their Application in Early Diagnosis of Cancers. Anal Cell Pathol (Amst). 2020;2020:6283796.

132. Nath PR, Pal-Nath D, Kaur S, Gangaplara A, Meyer TJ, Cam MC, et al. Loss of CD47 alters CD8+ T cell activation in vitro and immunodynamics in mice. OncoImmunology. 2022;11(1).

133. Yu L, Ding Y, Wan T, Deng T, Huang H, Liu J. Significance of CD47 and Its Association With Tumor Immune Microenvironment Heterogeneity in Ovarian Cancer. Frontiers in Immunology. 2021;12.

134. Yang M, Jiang C, Li L, Xing H, Hong L. Expression of CD47 in Endometrial Cancer and Its Clinicopathological Significance. J Oncol. 2022;2022:7188972.

135. Sun Y, Liang S, Li T, Peng C, Yang Y, Lin Y, et al. Prognostic implications of combined high expression of CD47 and MCT1 in breast cancer: a retrospective study during a 10-year period. Transl Cancer Res. 2022;11(1):29-42.

136. Benesova I, Capkova L, Ozaniak A, Pacas P, Kopeckova K, Galova D, et al. A comprehensive analysis of CD47 expression in various histological subtypes of soft tissue sarcoma: exploring novel opportunities for macrophage-directed treatments. Journal of Cancer Research and Clinical Oncology. 2024;150(3).

137. Pan Y, Lu F, Fei Q, Yu X, Xiong P, Yu X, et al. Single-cell RNA sequencing reveals compartmental remodeling of tumor-infiltrating immune cells induced by anti-CD47 targeting in pancreatic cancer. J Hematol Oncol. 2019;12(1):124.

138. Giatromanolaki A, Mitrakas A, Anestopoulos I, Kontosis A, Koukourakis IM, Pappa A, et al. Expression of CD47 and SIRPα Macrophage Immune-Checkpoint Pathway in Non-Small-Cell Lung Cancer. Cancers (Basel). 2022;14(7).

139. Pan L, Hu L, Chen M, Song Y, Chen Z, Gu Y, et al. A novel CD47-blocking peptide fused to pro-apoptotic KLA repeat inhibits lung cancer growth in mice. Cancer Immunology, Immunotherapy. 2023;72(12):4179-94.

140. Bates KM, Vathiotis I, Macneil T, Ahmed FS, Aung TN, Katlinskaya Y, et al. Spatial characterization and quantification of CD40 expression across cancer types. BMC Cancer. 2023;23(1).

141. Yan C, Richmond A. Hiding in the dark: pan-cancer characterization of expression and clinical relevance of CD40 to immune checkpoint blockade therapy. Molecular Cancer. 2021;20(1).

142. Liu G, Luo P. Targeting CD137 (4-1BB) towards improved safety and efficacy for cancer immunotherapy. Frontiers in Immunology. 2023;14.

143. Wu G, He M, Ren K, Ma H, Xue Q. Inducible Co-Stimulator ICOS Expression Correlates with Immune Cell Infiltration and Can Predict Prognosis in Lung Adenocarcinoma. International Journal of General Medicine. 2022;Volume 15:3739-51.

9. Bibliography of the candidate's publications

Cumulative impact factor: 22.5

9.1. List of publications that served as a basis for the current thesis

Csende K, Ferencz B, Boettiger K, Pozonec M D, Lantos A, Ferenczy A, Pipek O, Solta A, Ernhofer B, Laszlo V, Megyesfalvi E, Schelch K, Pozonec V, Skarda J, Skopelidou V, Lohinai Z, Lang C, Horvath Lilla, Dezso K, Fillinger J, Renyi-Vamos F, Aigner C, Dome B, Megyesfalvi Z
Comparative profiling of surgically resected primary tumors and their lymph node metastases in small-cell lung cancer
ESMO OPEN 10 : 4 Paper: 104514 , 10 p. (2025)
Közlemény: 36052800 | Szakcikk (Folyóiratcikk) | Tudományos
Scopus - Cancer Research SJR indikátor: D1
Scopus - Oncology SJR indikátor: D1
IF: 8,3

Ferencz Bence, Megyesfalvi Zsolt, **Csende Kristóf**, Fillinger János, Poór Valentin, Lantos András, Pipek Orsolya, Sólyom-Tisza Anna, Rényi-Vámos Ferenc, Schelch Karin, Lang Christian, Schwndenwein Anna, Boettiger Kristiina, László Viktória, Hoetzenecker Konrad, Döme Balázs, Berta Judit
Comparative expression analysis of immune-related markers in surgically resected lung neuroendocrine neoplasms
LUNG CANCER 181 Paper: 107263, 14 p. (2023)
Közlemény: 33999025 | Szakcikk (Folyóiratcikk) | Tudományos
Scopus - Pulmonary and Respiratory Medicine SJR indikátor: D1
Scopus - Cancer Research SJR indikátor: Q1
Scopus - Oncology SJR indikátor: Q1
IF: 4,5

DOI:10.14753/SE.2025.3289

9.2. Other publications

2025

Csaba Márton, Ghimessy Áron Kristóf, Radeczky Péter, Megyesfalvi Zsolt, Kocsis Ákos, Agócs László, Döme Balázs, Fehér Csaba, Török Klára, Mészáros László, Bogyó Levente, Gieszer Balázs, **Csende Kristóf**, Nagy Dóra, Tihanyi Hanna, Tarsoly Gábor, Lality Sára, Hartyánszky K István, Kass József, Vágvölgyi Attila, Lungu Victor, Szegedi Róbert, Yu Evelin, Gyenge Bernát, Afari Dániel, Köllő Arnold, Madurka Ildikó, Rényi-Vámos Ferenc

Három intézet összefogása a központi régió magas színvonalú mellkassebészeti ellátásának érdekében

ORVOSI HETILAP 166 : 6 pp. 203-209. (2025)

Közlemény: 35752112 | Összefoglaló cikk (Folyóiratcikk) | Tudományos

Scopus - Medicine (miscellaneous) SJR indikátor: Q4

IF: 0,9

2024

Ghimessy Áron, Radeczky Péter, Török Klára, Bogyó Levente, **Csende Kristóf**, Mészáros László, Gieszer Balázs, Tihanyi Hanna, Tarsoly Gábor, Csaba Márton, Lality Sára, Hartyánszky István Kázmér, Kocsis Ákos, Madurka Ildikó Agócs László, Rényi-Vámos Ferenc

Robotasszisztált műtétek helye a mellkassebészetben. Saját tapasztalatok

MAGYAR ONKOLÓGIA 68 : 3 pp. 223-228. (2024)

Közlemény: 35421985 | Szakcikk (Folyóiratcikk) | Tudományos

Scopus - Medicine (miscellaneous) SJR indikátor: Q4

Scopus - Oncology SJR indikátor: Q4

Csende Kristóf, Megyesfalvi Zsolt, Ferencz Bence, Fillinger János, Poór Valentin, Lantos András, Pipek Orsolya, Sólyom-Tisza Anna, Schelch Karin, Bogos Krisztina, Kocsis Ákos, Agócs László, Rényi-Vámos Ferenc, Lang Christian, Schwendenwein Anna, Boettiger Kristiina, László Viktória, Döme Balázs, Berta Judit

Immunológiai markerek expressziójának vizsgálata neuroendokrin tüdődaganatokban

MAGYAR ONKOLÓGIA 67 : 1. szupplementum pp. 18-18. (2023)

Közlemény: 34326594 | Absztrakt / Kivonat (Folyóiratcikk) | Tudományos

Ferencz Bence, Török Klára, Pipek Orsolya, Fillinger János, **Csende Kristóf**, Lantos András, Černeková Radoslava, Mitták Marcel, Škarda Jozef, Delongová Patricie, Megyesfalvi Evelyn, Schelch Karin, Lang Christian, Solta Anna, Boettiger Kristiina, Brcic Luka, Lindenmann Jörg, Rényi-Vámos Ferenc, Aigner Clemens, Berta Judit, Megyesfalvi Zsolt, Döme Balázs

Expression patterns of novel immunotherapy targets in intermediate- and high-grade lung neuroendocrine neoplasms

CANCER IMMUNOLOGY IMMUNOTHERAPY 73 : 6 Paper: 114 , 15 p. (2024)

Közlemény: 34839166 | Szakcikk (Folyóiratcikk) | Tudományos

Scopus - Medicine (miscellaneous) SJR indikátor: D1

Scopus - Cancer Research SJR indikátor: Q1

Scopus - Immunology SJR indikátor: Q1

Scopus - Immunology and Allergy SJR indikátor: Q1

Scopus - Oncology SJR indikátor: Q1

IF: 5,1

2021

Agócs László, Kocsis Ákos, Radeczky Péter, Ghimessy Áron, Gieszer Balázs, Török Klára, Bogyó Levente, Mészáros László, Tallósy Bernadett, **Csende Kristóf**, Tihanyi Hanna, Tarsoly Gábor, Ferencz Bence, Megyesfalvi Zsolt, Döme Balázs, Rényi-Vámos Ferenc

VATS és nyílt torakotómia hatásai a posztoperatív szakra és a túlélésre

MAGYAR ONKOLÓGIA 65 : Suppl.1 pp. 7-7. (2021)

Közlemény: 32538135 | Absztrakt / Kivonat (Folyóiratcikk) | Tudományos

Ghimessy Áron, Gellért Áron, **Csende Kristóf**, Gieszer Balázs, Bogyó Levente, Radeczky Péter, Kocsis Ákos, Agócs László, Fillinger János, Alexis Slama, Megyesfalvi Zsolt, Rényi-Vámos Ferenc, Madurka Ildikó, Döme Balázs

Izolált tüdőperfúziós kísérleti modell használata farmakológiai ágensekkel sebészileg eltávolított tumoros tüdőkön

MAGYAR ONKOLÓGIA 65 : Suppl.1 pp. 21-22. (2021)

Közlemény: 32541123 | Absztrakt / Kivonat (Folyóiratcikk) | Tudományos

2019

Ghimessy Áron K, Farkas Attila, Gieszer Balázs, Radeczky Péter, **Csende Kristóf** Mészáros László, Török Klára, Fazekas Levente, Agócs László, Kocsis Ákos, Bartók Tibor, Dancs Tamás, Tóth Krisztina Kormosoi, Schönauer Nóra, Madurka Ildikó, Elek Jenő, Döme Balázs, Rényi-Vámos Férenc, Lang György, Taghavi Shahrokh, Hötzenecker Konrad, Klepetko Walter, Bogyó Levente
Donation After Cardiac Death, a Possibility to Expand the Donor Pool: Review and the Hungarian Experience
TRANSPLANTATION PROCEEDINGS 51 : 4 pp. 1276-1280. (2019)
Közlemény: 30687822 | Szakcikk (Folyóiratcikk) | Tudományos
Scopus - Surgery SJR indikátor: Q3
Scopus - Transplantation SJR indikátor: Q3
IF: 0,784

Gieszer Balázs, Radeczky Péter, Farkas Attila, Csende Kristóf, Mészáros László, Török Klára, Fazekas Levente, Bogyó Levente, Agócs László, Kocsis Ákos, Varga János, Bartók Tibor, Dancs Tamás, Kormosoi Tóth Krisztina, Schönauer Nóra, Madurka Ildikó, Elek Jenö, Döme Balázs, Rényi-Vámos Ferenc, Lang György Jaksch Péter, Ghimessy Áron K
Lung Transplant Patients on Kilimanjaro
TRANSPLANTATION PROCEEDINGS 51 : 4 pp. 1258-1262. (2019)
Közlemény: 30687823 | Szakcikk (Folyóiratcikk) | Tudományos
Scopus - Surgery SJR indikátor: Q3
Scopus - Transplantation SJR indikátor: Q3
IF: 0,784

Gieszer Balázs, Ghimessy Áron, Radeczky Péter, Farkas Attila, Csende Kristóf, Bogyó Levente, Fazekas Levente, Kovács Nóra, Madurka Ildikó, Kocsis Ákos, Agócs László, Török Klára, Bartók Tibor, Dancs Tamás, Schönauer Nóra, Tóth Kriszta, Eszes Noémi, Bohács Anikó, Czebe Krisztina, Csiszér Eszter, Mihály Sándor, Kovács Lajos, Müller Veronika, Elek Jenő, Rényi-Vámos Ferenc, Lang György
First 3 Years of the Hungarian Lung Transplantation Program

TRANSPLANTATION PROCEEDINGS 51 : 4 pp. 1254-1257. (2019)
Közlemény: 30687824 | Szakcikk (Folyóiratcikk) | Tudományos
Scopus - Surgery SJR indikátor: Q3
Scopus - Transplantation SJR indikátor: Q3
IF: 0,784

Radeczky P, Ghimessy Á K, Farkas A, **Csende K**, Mészáros L, Török K, Fazekas L, Agócs L, Kocsis Á, Bartók T, Dancs T, Tóth K K, Schönauer N, Bogyó L, Bohács A, Madurka I, Elek J, Döme B, Rényi-Vámos F, Lang G, Gieszer B
Antibody-Mediated Rejection in a Multiple Lung Transplant Patient: A Case Report
TRANSPLANTATION PROCEEDINGS 51 : 4 pp. 1296-1298. (2019)
Közlemény: 30687843 | Rövid közlemény (Folyóiratcikk) | Tudományos
Scopus - Surgery SJR indikátor: Q3
Scopus - Transplantation SJR indikátor: Q3
IF: 0,784

2018

Gieszer Balázs, Radeczky Péter, Ghimessy Áron, Farkas Attila, **Csende Kristóf**, Bogyó Levente, Fazekas Levente, Kovács Nóra, Madurka Ildikó, Kocsis Ákos, Agócs László, Török Klára, Bartók Tibor, Dancs Tamás, Schönauer Nóra, Tóth Krisztina, Szabó József, Eszes Noémi, Bohács Anikó, Czebe Krisztina, Csiszér Eszter, Mihály Sándor, Kovács Lajos, Müller Veronika, Elek Jenő, Rényi-Vámos Ferenc, Lang György
A magyar tüdőtranszplantációs program indulása és első eredményei [The start of the Hungarian lung transplantation program and the first results]
ORVOSI HETILAP 159 : 46 pp. 1859-1868. (2018)
Közlemény: 30321209 | Összefoglaló cikk (Folyóiratcikk) | Tudományos
Scopus - Medicine (miscellaneous) SJR indikátor: Q3
IF: 0,564

DOI:10.14753/SE.2025.3289

10. Acknowledgments

I would like to express my sincere appreciation to my supervisors and mentors, Dr. Zsolt Megyesfalvi and Professor Balázs Döme, whose guidance and support were indispensable throughout my PhD project.

My heartfelt thanks also go to Professor Ferenc Rényi-Vámos, Head of the Department of Thoracic Surgery, whose support was essential during our research.

I am deeply grateful to General Directors Krisztina Bogos, Professor Magdolna Dank, and Professor Csaba Polgár for all the help they have provided to our Team.

I would like to extend special thanks to Dr. Bence Ferencz, Dr. Judit Berta, and Dr. János Fillinger for their contributions during this journey

I am also grateful to all my colleagues from the National Institute of Oncology and Semmelweis University who helped me become a thoracic surgeon: Dr. Agócs László, Dr. Ghimessy Áron, Dr. Kocsis Ákos, Dr. Török Klára, Dr. Bogyó Levente, Dr. Mészáros László, Dr. Gieszer Balázs, Dr. Radeczky Péter, Dr. Tallósy Bernadett, Dr. Tihanyi Hanna, Dr. Tarsoly Gábor, Dr. Csaba Márton, Dr. Lality Sára, Dr. Hartyánszky István.
Thank you for your dedication, perseverance, and the tireless work we shared over the past years.
I am especially thankful to Dr. Áron Ghimessy, who not only helped me throughout my residency as a colleague but also as a friend.

Thanks should also go to my colleagues from the Medical University of Vienna and the National Korányi Institute of Pulmonology: Erzsébet Schlegl, Erzsébet Nagy, Szilvia Török, Anita Rózsás, Lilla Horváth, Vivien Téglás, Mária Dorothea Pozonec, Orsolya Pipek.
I would like to take a moment to express my gratitude to our collaborators from around the world and the patients who participated in our studies. Their invaluable

DOI:10.14753/SE.2025.3289

contributions, along with our collective efforts, rendered our studies possible, underscoring the collaborative nature of our research.

Finally, I would also like to express my gratitude to my whole family, without whom I would most certainly not be here today. Their support and sacrifices have been the cornerstone of my journey. I would like to express my gratitude to my wife, Petra, for her unwavering support, and to my daughter, who has been a constant source of joy. I am truly indebted to my parents, who have always believed in me.

Thank you all for your support and encouragement!